

**NIST Technical Note  
NIST TN 2274**

**Partial Elastic Shape Registration of  
3D Surfaces using Dynamic  
Programming**

Javier Bernal  
Jim Lawrence

This publication is available free of charge from:  
<https://doi.org/10.6028/NIST.TN.2274>

**NIST Technical Note  
NIST TN 2274**

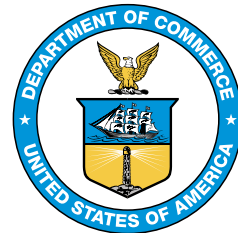
**Partial Elastic Shape Registration of  
3D Surfaces using Dynamic  
Programming**

Javier Bernal  
*Information Technology Laboratory  
Applied and Computational Mathematics Division*

Jim Lawrence  
*George Mason University  
Information Technology Laboratory  
Applied and Computational Mathematics Division*

This publication is available free of charge from:  
<https://doi.org/10.6028/NIST.TN.2274>

November 2023



U.S. Department of Commerce  
*Gina M. Raimondo, Secretary*

National Institute of Standards and Technology  
*Laurie E. Locascio, NIST Director and Under Secretary of Commerce for Standards and Technology*

Certain commercial equipment, instruments, or materials, commercial or non-commercial, are identified in this paper in order to specify the experimental procedure adequately. Such identification does not imply recommendation or endorsement of any product or service by NIST, nor does it imply that the materials or equipment identified are necessarily the best available for the purpose.

#### **NIST Technical Series Policies**

[Copyright, Use, and Licensing Statements](#)

[NIST Technical Series Publication Identifier Syntax](#)

#### **Publication History**

Approved by the NIST Editorial Review Board on 2023-10-26

#### **How to cite this NIST Technical Series Publication:**

Javier Bernal, Jim Lawrence (2023) Partial Elastic Shape Registration of 3D Surfaces using Dynamic Programming. (National Institute of Standards and Technology, Gaithersburg, MD), NIST TN 2274.  
<https://doi.org/10.6028/NIST.TN.2274>

#### **NIST Author ORCID iDs**

Javier Bernal: 0000-0002-9681-7007

Jim Lawrence: 0000-0003-0638-2559

#### **Contact Information**

[javier.bernal@nist.gov](mailto:javier.bernal@nist.gov)

## **Abstract**

The computation of the elastic shape registration of two simple surfaces in 3–dimensional space and therefore of the elastic shape distance between them has been investigated by Kurtek, Jermyn, et al. who have proposed algorithms to carry out this computation. These algorithms accomplish this by minimizing a distance function between the surfaces in terms of rotations and reparametrizations of one of the surfaces, the optimization over reparametrizations using a gradient approach that may produce a local solution. Now minimizing in terms of rotations and a special subset of the set of reparametrizations, we propose an algorithm for minimizing the distance function, the optimization over reparametrizations based on dynamic programming. This approach does not necessarily produce an optimal solution for the registration and distance problem, but perhaps a solution closer to optimal than the local solution that an algorithm with a gradient approach for optimizing over the entire set of reparametrizations may produce. In fact we propose that when computing the elastic shape registration of two simple surfaces and the elastic shape distance between them with an algorithm based on a gradient approach for optimizing over the entire set of reparametrizations, to use as the input initial solution the optimal rotation and reparametrization computed with our proposed algorithm.

## **Keywords**

dynamic programming; elastic shape distance; homeomorphism; rotation matrix; shape analysis; singular value decomposition.

## Table of Contents

1. Introduction	1
2. Homeomorphisms and the Area of a Surface	3
3. The Shape Function of a Parametrized Surface	6
4. The Elastic Shape Distance between Surfaces	9
5. Computation of Homeomorphism for Partial Registration of Surfaces using Dynamic Programming	11
6. Computation of Rotation Matrix for Rigid Alignment of Surfaces	14
7. Procedure for Optimizing over both Rotations and Reparametrizations using Dynamic Programming	16
8. Results from Implementation of Methods	18
9. Summary	29
References	30

## List of Figures

Fig. 1.	Two views of the boundaries of the same two surfaces in 3-dimensional space, each of sinusoidal shape. Their shapes are essentially identical; thus the elastic shape distance between them should be essentially zero.	2
Fig. 2.	Three plots of boundaries of surfaces of the sine kind. A partial elastic shape registration of the two surfaces in each plot and the elastic shape distance between them associated with the registration were computed.	21
Fig. 3.	Graphs of optimal diffeomorphisms from execution of Dynamic Programming software on the three pairs of surfaces with $\gamma(r,t) = (r^{5/4}, t)$ , $(r,t) \in [0,1] \times [0,1]$ . One per pair, as for each pair the same two curves in 3-d space were used as input to the software each time it was executed. Thus the same diffeomorphism was computed each time for each pair of surfaces.	22
Fig. 4.	With $\gamma(r,t) = (r^{5/4}, t)$ , $(r,t) \in [0,1] \times [0,1]$ , views of boundaries of pair of surfaces in the rightmost plot in Figure 2 before computation of partial elastic shape registration (leftmost plot here), of boundary of optimally rotated first surface (middle plot), and of boundary of optimally reparametrized second surface (rightmost plot) after computations.	23
Fig. 5.	For $\gamma(r,t) = (r^{5/4}, t^{5/4})$ , $(r,t) \in [0,1] \times [0,1]$ , views of graph of optimal diffeomorphism computed the 51 <sup>st</sup> time the Dynamic Programming software was executed (leftmost plot), of boundary of optimally rotated first surface (middle plot), and of optimally reparametrized second surface (rightmost plot) after computation of partial elastic shape registration.	23
Fig. 6.	Boundaries of two surfaces of similar shape of the helicoid kind for $k = 4$ , type 1 in red, type 2 in blue.	24

- Fig. 7. For  $\gamma(r,t) = (r^{5/4}, t)$ ,  $(r,t) \in [0, 1] \times [0, 1]$ , views of graph of optimal diffeomorphism computed each time the Dynamic Programming software was executed on pair of surfaces (leftmost plot), of boundary of optimally rotated first surface (middle plot), and of optimally reparametrized second surface (rightmost plot) after computation of partial elastic shape registration. 25
- Fig. 8. For  $\gamma(r,t) = (r^{5/4}, t^{5/4})$ ,  $(r,t) \in [0, 1] \times [0, 1]$ , views of graph of optimal diffeomorphism computed the 51<sup>st</sup> time the Dynamic Programming software was executed (leftmost plot), of boundary of optimally rotated first surface (middle plot), and of optimally reparametrized second surface (rightmost plot) after computation of partial elastic shape registration. 26
- Fig. 9. Boundaries of two surfaces of similar shape of the cosine-sine kind, type 1 in red, type 2 in blue. 27
- Fig. 10. For  $\gamma(r,t) = (r^{5/4}, t)$ ,  $(r,t) \in [0, 1] \times [0, 1]$ , views of graph of optimal diffeomorphism computed the 51<sup>st</sup> time the Dynamic Programming software was executed on pair of surfaces (leftmost plot), of boundary of optimally rotated first surface (middle plot), and of optimally reparametrized second surface (rightmost plot) after computation of partial registration. 28
- Fig. 11. For  $\gamma(r,t) = (r^{5/4}, t^{5/4})$ ,  $(r,t) \in [0, 1] \times [0, 1]$ , views of graph of optimal diffeomorphism computed the 51<sup>st</sup> time the Dynamic Programming software was executed (leftmost plot), of boundary of optimally rotated first surface (middle plot), and of optimally reparametrized second surface (rightmost plot) after computation of partial elastic shape registration. 28









$h(D) \setminus h(p)$  is simply connected as well so that  $h(p)$  cannot be in the interior of  $h(D)$ , thus must be in its boundary. On the other hand, if  $q$  is in the boundary of  $h(D)$ , then through a similar argument since  $q$  is in  $h(D)$  ( $h(D)$  is closed), it can be shown that  $h^{-1}(q)$  is in the boundary of  $h^{-1}(h(D)) = D$ . Thus  $h$  maps the boundary of  $D$  to exactly the boundary of  $h(D)$ .  $\square$

In what follows, given a surface  $S$  in 3–dimensional space, elementary regions  $D, E$  in  $\mathbb{R}^2$ , and one-to-one functions  $c, p$  of class  $C^1$ ,  $c : D \rightarrow \mathbb{R}^3$ ,  $p : E \rightarrow \mathbb{R}^3$ ,  $c(D) = S$ ,  $p(E) = S$ , so that  $c$  and  $p$  are parametrizations of  $S$  with domain  $D$  and  $E$ , respectively, we say  $p$  is a *reparametrization* of  $c$  or that  $p$  *reparametrizes*  $S$  (given as an image of  $c$ ), if  $p = c \circ h$  for a  $C^1$  homeomorphism  $h$  from  $E$  onto  $D$ . For  $(u, v)$  in  $D$ , writing  $c(u, v) = (x(u, v), y(u, v), z(u, v))$ , then given a point  $(u_0, v_0)$  in  $D$ , the vector tangent to the surface  $S$  at  $c(u_0, v_0)$  in the  $u$  direction is given by

$$\frac{\partial c}{\partial u}(u_0, v_0) = \left( \frac{\partial x}{\partial u}(u_0, v_0), \frac{\partial y}{\partial u}(u_0, v_0), \frac{\partial z}{\partial u}(u_0, v_0) \right),$$

and in the  $v$  direction by

$$\frac{\partial c}{\partial v}(u_0, v_0) = \left( \frac{\partial x}{\partial v}(u_0, v_0), \frac{\partial y}{\partial v}(u_0, v_0), \frac{\partial z}{\partial v}(u_0, v_0) \right).$$

We say the surface  $S$  is *regular* (relative to the parametrization  $c$ ) if at every point  $c(u_0, v_0)$  in  $S$  the cross product  $\frac{\partial c}{\partial u}(u_0, v_0) \times \frac{\partial c}{\partial v}(u_0, v_0)$  is nonzero. We note that if  $S$  is regular, then at every point  $c(u_0, v_0)$  in  $S$ ,  $\frac{\partial c}{\partial u}(u_0, v_0) \times \frac{\partial c}{\partial v}(u_0, v_0)$  is a nonzero vector normal to  $S$  at  $c(u_0, v_0)$ .

With  $c, D, S, \frac{\partial c}{\partial u}(u_0, v_0), \frac{\partial c}{\partial v}(u_0, v_0)$  as above,  $S$  regular (relative to  $c$ ), the surface area  $A(S)$  of the parametrized surface  $S$  is given by

$$A(S) = \int \int_D \left\| \frac{\partial c}{\partial u}(u, v) \times \frac{\partial c}{\partial v}(u, v) \right\| du dv$$

where  $\|\cdot\|$  is the 3-dimensional Euclidean norm.

With  $c, D, p, E, S, \frac{\partial c}{\partial u}(u_0, v_0), \frac{\partial c}{\partial v}(u_0, v_0), h$  as above so that  $p$  is also a parametrization of  $S$  with domain  $E$ , and  $p$  is a reparametrization of  $c$ ,  $p = c \circ h$ , the result that follows shows the surface area  $A(S)$  of  $S$  does not change if it is computed with the parametrization  $p$  of  $S$  with domain  $E$  instead of the parametrization  $c$  of  $S$  with domain  $D$ . For  $(r, t)$  in  $E$ , writing  $h(r, t) = (u(r, t), v(r, t))$ , and letting  $\frac{\partial(u, v)}{\partial(r, t)}$  be the determinant of the Jacobian of  $h$ ,  $\frac{\partial(u, v)}{\partial(r, t)}$  is assumed to be nonzero on  $E$ . Finally, for  $(r, t)$  in  $E$ , writing  $p(r, t) = (\hat{x}(r, t), \hat{y}(r, t), \hat{z}(r, t))$ , then given a point  $(r_0, t_0)$  in  $E$ , the vector tangent to the surface  $S$  at  $p(r_0, t_0)$  in the  $r$  direction is given by

$$\frac{\partial p}{\partial r}(r_0, t_0) = \left( \frac{\partial \hat{x}}{\partial r}(r_0, t_0), \frac{\partial \hat{y}}{\partial r}(r_0, t_0), \frac{\partial \hat{z}}{\partial r}(r_0, t_0) \right),$$

and in the  $t$  direction by

$$\frac{\partial p}{\partial t}(r_0, t_0) = \left( \frac{\partial \hat{x}}{\partial t}(r_0, t_0), \frac{\partial \hat{y}}{\partial t}(r_0, t_0), \frac{\partial \hat{z}}{\partial t}(r_0, t_0) \right).$$

**Theorem 3:** Given  $c, D, p, E, S, \frac{\partial c}{\partial u}(u_0, v_0), \frac{\partial c}{\partial v}(u_0, v_0), \frac{\partial p}{\partial r}(r_0, t_0), \frac{\partial p}{\partial t}(r_0, t_0), h, \frac{\partial(u,v)}{\partial(r,t)}$  as above, then  $S$  is regular relative to  $p$  and

$$\int \int_E \left\| \frac{\partial p}{\partial r}(r, t) \times \frac{\partial p}{\partial t}(r, t) \right\| dr dt = \int \int_D \left\| \frac{\partial c}{\partial u}(u, v) \times \frac{\partial c}{\partial v}(u, v) \right\| du dv.$$

**Proof:** With  $(u(r, t), v(r, t)) = h(r, t)$ , then

$$p(r, t) = c(h(r, t)) = c(u(r, t), v(r, t)),$$

so that

$$\frac{\partial p}{\partial r} = \frac{\partial c}{\partial u} \frac{\partial u}{\partial r} + \frac{\partial c}{\partial v} \frac{\partial v}{\partial r}, \quad \frac{\partial p}{\partial t} = \frac{\partial c}{\partial u} \frac{\partial u}{\partial t} + \frac{\partial c}{\partial v} \frac{\partial v}{\partial t}.$$

Thus

$$\begin{aligned} \frac{\partial p}{\partial r} \times \frac{\partial p}{\partial t} &= \left( \frac{\partial c}{\partial u} \frac{\partial u}{\partial r} + \frac{\partial c}{\partial v} \frac{\partial v}{\partial r} \right) \times \left( \frac{\partial c}{\partial u} \frac{\partial u}{\partial t} + \frac{\partial c}{\partial v} \frac{\partial v}{\partial t} \right) \\ &= \left( \frac{\partial c}{\partial u} \times \frac{\partial c}{\partial v} \right) \left( \frac{\partial u}{\partial r} \frac{\partial v}{\partial t} \right) + \left( \frac{\partial c}{\partial v} \times \frac{\partial c}{\partial u} \right) \left( \frac{\partial v}{\partial r} \frac{\partial u}{\partial t} \right) \\ &= \left( \frac{\partial c}{\partial u} \times \frac{\partial c}{\partial v} \right) \left( \frac{\partial u}{\partial r} \frac{\partial v}{\partial t} - \frac{\partial v}{\partial r} \frac{\partial u}{\partial t} \right) \\ &= \left( \frac{\partial c}{\partial u} \times \frac{\partial c}{\partial v} \right) \frac{\partial(u, v)}{\partial(r, t)} \end{aligned}$$

so that  $S$  is regular relative to  $p$  since both  $\frac{\partial c}{\partial u} \times \frac{\partial c}{\partial v}$  and  $\frac{\partial(u,v)}{\partial(r,t)}$  are nonzero on  $E$ , and

$$\begin{aligned} \int \int_E \left\| \frac{\partial p}{\partial r} \times \frac{\partial p}{\partial t} \right\| dr dt &= \int \int_E \left\| \left( \frac{\partial c}{\partial u} \times \frac{\partial c}{\partial v} \right) \frac{\partial(u, v)}{\partial(r, t)} \right\| dr dt \\ &= \int \int_E \left\| \frac{\partial c}{\partial u} \times \frac{\partial c}{\partial v} \right\| \left| \frac{\partial(u, v)}{\partial(r, t)} \right| dr dt \\ &= \int \int_D \left\| \frac{\partial c}{\partial u} \times \frac{\partial c}{\partial v} \right\| du dv \end{aligned}$$

by the change of variables formula. □

### 3. The Shape Function of a Parametrized Surface

In this section we define the shape function of a parametrized surface in 3-dimensional space and present some fundamental results about this function. A similar definition and similar results have been presented in [2, 4, 7, 14, 15] in the context of the shape function of a parametrized curve in  $d$ -dimensional space,  $d$  any positive integer. Accordingly, in [2, 4, 7, 14, 15], given  $\beta : [0, 1] \rightarrow \mathbb{R}^d$  of class  $C^1$ , a parametrization of a curve in  $\mathbb{R}^d$ , the shape function  $q$  of  $\beta$ , i.e., the shape function  $q$  of the curve that  $\beta$  parametrizes relative to  $\beta$ ,  $q : [0, 1] \rightarrow \mathbb{R}^d$ , is defined by  $q(t) = \dot{\beta}(t) / \sqrt{\|\dot{\beta}(t)\|}$ ,  $t \in [0, 1]$  ( $d$ -dimensional 0 if  $\dot{\beta}(t)$  equals  $d$ -dimensional 0). It follows then that  $q$  is square integrable as

$$\int_0^1 \|q(t)\|^2 dt = \int_0^1 \|\dot{\beta}(t) / \sqrt{\|\dot{\beta}(t)\|}\|^2 dt = \int_0^1 \|\dot{\beta}(t)\| dt$$

which is the length of the curve that  $\beta$  parametrizes, where  $\|\cdot\|$  is the  $d$ -dimensional Euclidean norm. Note that in what follows we ignore the usual definition of a diffeomorphism and refer to homeomorphisms on  $[0, 1]$  as diffeomorphisms in order to distinguish them from homeomorphisms on elementary regions in the plane. Again with  $q$  the shape function of  $\beta$  and  $\Gamma$  the set of  $C^1$  orientation-preserving diffeomorphisms of  $[0, 1]$  so that for  $\gamma \in \Gamma$  then  $\dot{\gamma} \geq 0$  on  $[0, 1]$ , it then follows that for  $\gamma \in \Gamma$  the shape function of the reparametrization  $\beta \circ \gamma$  of  $\beta$  is  $(q, \gamma) = (q \circ \gamma) \sqrt{\dot{\gamma}}$ . With  $\|q\|_2 = (\int_0^1 \|q(t)\|^2 dt)^{1/2}$ , we also note that given  $\beta_1, \beta_2 : [0, 1] \rightarrow \mathbb{R}^d$  of class  $C^1$ , parametrizations of curves in  $\mathbb{R}^d$  with shape functions  $q_1, q_2$ , respectively, then  $\|(q_1, \gamma) - (q_2, \gamma)\|_2 = \|q_1 - q_2\|_2$  for any  $\gamma \in \Gamma$ , and from this, with  $\Gamma_0 = \{\gamma \in \Gamma, \dot{\gamma} > 0 \text{ on } [0, 1]\}$ , it has been demonstrated [2, 14] that ignoring rotations, the number  $\inf_{\gamma \in \Gamma_0} \|q_1 - (q_2, \gamma)\|_2$  can then be used as a well-defined distance between the two curves that  $\beta_1, \beta_2$  parametrize,  $\beta_1$  and  $\beta_2$  both normalized to parametrize curves of length 1.

With  $c, D, S, \frac{\partial c}{\partial u}, \frac{\partial c}{\partial v}$  as in the previous section,  $S$  regular (relative to  $c$ ), following the idea of the definition of the shape function of a parametrized curve in  $d$ -dimensional space as described above, we define the shape function  $q$  of the parametrization  $c$  of  $S$  with domain  $D$ , i.e., the shape function  $q$  of the surface  $S$  relative to its parametrization  $c$  with domain  $D$ ,  $q : D \rightarrow \mathbb{R}^3$ , so that

$$\int \int_D \|q(u, v)\|^2 du dv = \int \int_D \left\| \frac{\partial c}{\partial u} \times \frac{\partial c}{\partial v} \right\| du dv$$

which is the surface area of  $S$ . This is easily seen to be indeed the case if we define the shape function  $q$  of  $c$  on  $D$  by

$$q = \left( \frac{\partial c}{\partial u} \times \frac{\partial c}{\partial v} \right) / \sqrt{\left\| \frac{\partial c}{\partial u} \times \frac{\partial c}{\partial v} \right\|}.$$

We do define  $q$  this way and note that this definition of the shape function of a surface relative to a parametrization of the surface, is slightly different from the one in [10] but similar to the one in [6]. We also note that if we allow  $\frac{\partial c}{\partial u} \times \frac{\partial c}{\partial v}$  to be 3–dimensional zero at certain points, then  $q$  is defined to be 3–dimensional zero at those points.

With  $c, q, D, S$  as above, the following result, similar to the one mentioned above in the context of the shape function of the parametrization of a curve in  $d$ –dimensional space, shows how to compute the shape function of a reparametrization of  $c$  from the shape function  $q$  of  $c$ . Here  $p$  is the reparametrization of  $c$ , i.e., for an elementary region  $E$  in  $\mathbb{R}^2$ ,  $p$  is a parametrization of  $S$  with domain  $E$ , and  $p = c \circ h$  for a  $C^1$  homeomorphism  $h$  from  $E$  onto  $D$ . Assuming  $\frac{\partial(u,v)}{\partial(r,t)} \geq 0$  on  $E$ ,  $\frac{\partial(u,v)}{\partial(r,t)}$  the determinant of the Jacobian of  $h$ , we define a function on  $E$  into  $\mathbb{R}^3$ , which we denote by  $(q, h)$ , as follows:

$$(q, h) \equiv (q \circ h) \sqrt{\frac{\partial(u,v)}{\partial(r,t)}}.$$

**Theorem 4:** Given  $c, q, D, p, h, E, S, \frac{\partial(u,v)}{\partial(r,t)}$  as above, the shape function on  $E$  of the reparametrization  $p = c \circ h$  of  $c$  is then  $(q, h)$ .

**Proof:** With  $(u(r,t), v(r,t)) = h(r,t)$ , so that

$$p(r,t) = c(h(r,t)) = c(u(r,t), v(r,t)),$$

then on  $E$ , as established in the proof of Theorem 3, we have

$$\frac{\partial p}{\partial r} \times \frac{\partial p}{\partial t} = \left( \frac{\partial c}{\partial u} \times \frac{\partial c}{\partial v} \right) \frac{\partial(u,v)}{\partial(r,t)}.$$

Thus, if  $\hat{q}$  is the shape function of  $p$  on  $E$ , from the definition of a shape function it must then be that

$$\begin{aligned} \hat{q} &= \left( \frac{\partial p}{\partial r} \times \frac{\partial p}{\partial t} \right) / \sqrt{\left\| \frac{\partial p}{\partial r} \times \frac{\partial p}{\partial t} \right\|} \\ &= \left( \frac{\partial c}{\partial u} \times \frac{\partial c}{\partial v} \right) \frac{\partial(u,v)}{\partial(r,t)} / \sqrt{\left\| \left( \frac{\partial c}{\partial u} \times \frac{\partial c}{\partial v} \right) \frac{\partial(u,v)}{\partial(r,t)} \right\|} \\ &= \left( \left( \frac{\partial c}{\partial u} \times \frac{\partial c}{\partial v} \right) / \sqrt{\left\| \frac{\partial c}{\partial u} \times \frac{\partial c}{\partial v} \right\|} \right) \sqrt{\frac{\partial(u,v)}{\partial(r,t)}} \\ &= (q \circ h) \sqrt{\frac{\partial(u,v)}{\partial(r,t)}} = (q, h). \end{aligned}$$

□

Other results about shape functions of parametrized surfaces, similar to results about shape functions of parametrized curves in  $d$ -dimensional space [2, 14], can be developed. Given  $c, q, p, h, D, E, S, \frac{\partial(u,v)}{\partial(r,t)}$  as above,  $q$  the shape function of  $c$ ,  $p = c \circ h$ ,  $h$  a  $C^1$  homeomorphism from  $E$  onto  $D$ ,  $\frac{\partial(u,v)}{\partial(r,t)}$  the determinant of the Jacobian of  $h$ , assuming now  $\frac{\partial(u,v)}{\partial(r,t)} > 0$  on  $E$ , so that  $\frac{\partial(r,t)}{\partial(u,v)}(u,v) = \left(\frac{\partial(u,v)}{\partial(r,t)}(r,t)\right)^{-1}$ ,  $\frac{\partial(r,t)}{\partial(u,v)}$  the determinant of the Jacobian of  $h^{-1}$  on  $D$ , then with  $(q, h)$  as defined above, one such result is that  $((q, h), h^{-1}) = q$  on  $D$ . This result together with the theorem that follows are of importance in the next section for justifying the definition of the distance between surfaces in a manner similar to the way the definition of the distance between curves in  $d$ -dimensional space is justified [2, 14]. The theorem shows homeomorphisms act by isometries on shape functions of parametrized surfaces.

**Theorem 5:** Given  $D, E, h, \frac{\partial(u,v)}{\partial(r,t)}$  as above,  $\frac{\partial(u,v)}{\partial(r,t)} \geq 0$  on  $E$ ;  $S_1, S_2$  surfaces,  $c_1, c_2$  parametrizations of  $S_1, S_2$ , respectively, both with domain  $D$ ;  $p_1, p_2$  parametrizations of  $S_1, S_2$ , respectively, both with domain  $E$ ;  $p_1, p_2$  reparametrizations of  $c_1, c_2$ , respectively,  $p_1 = c_1 \circ h, p_2 = c_2 \circ h$ ;  $q_1, q_2, \hat{q}_1, \hat{q}_2$  the shape functions of  $c_1, c_2, p_1, p_2$ , respectively, then

$$\begin{aligned} \|\hat{q}_1 - \hat{q}_2\|_{2,E} &\equiv \left( \int \int_E \|\hat{q}_1 - \hat{q}_2\|^2 dr dt \right)^{1/2} \\ &= \left( \int \int_D \|q_1 - q_2\|^2 du dv \right)^{1/2} \\ &\equiv \|q_1 - q_2\|_{2,D}. \end{aligned}$$

**Proof:** From Theorem 4,  $\hat{q}_1 = (q_1, h), \hat{q}_2 = (q_2, h)$ , thus

$$\begin{aligned} \|\hat{q}_1 - \hat{q}_2\|_{2,E}^2 &= \int \int_E \|\hat{q}_1 - \hat{q}_2\|^2 dr dt \\ &= \int \int_E \|(q_1, h) - (q_2, h)\|^2 dr dt \\ &= \int \int_E \|(q_1 \circ h) \sqrt{\frac{\partial(u,v)}{\partial(r,t)}} - (q_2 \circ h) \sqrt{\frac{\partial(u,v)}{\partial(r,t)}}\|^2 dr dt \\ &= \int \int_E \|(q_1 \circ h) - (q_2 \circ h)\|^2 \frac{\partial(u,v)}{\partial(r,t)} dr dt \\ &= \int \int_D \|q_1 - q_2\|^2 du dv \\ &= \|q_1 - q_2\|_{2,D}^2 \end{aligned}$$

by the change of variables formula. □

#### 4. The Elastic Shape Distance between Surfaces

In this section we define and justify the elastic shape distance between two surfaces of unit area. This is done at first in terms of  $C^1$  homeomorphisms with Jacobians of positive determinant (each homeomorphism defines a reparametrization of one of the surfaces), and later in terms of rotations as well. Given that  $S_1$  and  $S_2$  are the two surfaces, we assume they are simple and are parametrized by functions with the same domain, i.e., an elementary region  $D$  in the  $xy$  plane exists together with parametrizations  $c_1$  and  $c_2$  with domain  $D$  of  $S_1$  and  $S_2$ , respectively,  $c_1 : D \rightarrow \mathbb{R}^3$ ,  $c_2 : D \rightarrow \mathbb{R}^3$ ,  $S_1 = c_1(D)$ ,  $S_2 = c_2(D)$ . Letting  $\Sigma_0$  be the set of all  $C^1$  homeomorphisms  $h$ , from  $D$  onto  $D$ , with  $\frac{\partial(u,v)}{\partial(r,t)} > 0$  on  $D$ ,  $\frac{\partial(u,v)}{\partial(r,t)}$  the determinant of the Jacobian of  $h$ , given that  $q_1$  and  $q_2$  are, respectively, the shape functions of  $c_1$  and  $c_2$ , then using arguments similar to arguments for justifying the definition of the distance between curves in  $d$ -dimensional space found in [2, 14], ignoring rotations, it can be demonstrated that the number

$$\begin{aligned} \inf_{h \in \Sigma_0} \|q_1 - (q_2, h)\|_{2,D} &= \inf_{h \in \Sigma_0} \left( \int \int_D \|q_1 - (q_2, h)\|^2 dr dt \right)^{1/2} = \\ &= \inf_{h \in \Sigma_0} \left( \int \int_D \|q_1 - (q_2 \circ h)\|^2 \sqrt{\frac{\partial(u,v)}{\partial(r,t)}} dr dt \right)^{1/2} \end{aligned}$$

can be used as a well-defined distance between the surfaces  $S_1$  and  $S_2$ ,  $c_1$  and  $c_2$  both normalized to parametrize surfaces of area equal to 1. Note that the arguments for justifying this definition of the distance between the two surfaces are in part based on Theorem 5 in the previous section and the result described in the paragraph preceding Theorem 5.

That rotations as well act by isometries on shape functions of parametrized surfaces is justified as follows. With  $q_1, q_2$  as above, assuming  $R$  is a 3-dimensional rotation matrix, i.e.,  $R \in SO(3)$ ,  $SO(3)$  the group of  $3 \times 3$  orthogonal matrices of determinant equal to 1, then because  $R$  is orthogonal, it follows easily that

$$\begin{aligned} \|Rq_1 - Rq_2\|_{2,D} &= \left( \int \int_D \|Rq_1 - Rq_2\|^2 dudv \right)^{1/2} \\ &= \left( \int \int_D \|q_1 - q_2\|^2 dudv \right)^{1/2} \\ &= \|q_1 - q_2\|_{2,D}. \end{aligned}$$

Also as established in [14] for shape functions of parametrized curves in  $d$ -dimensional space, it follows by similar arguments that given  $h \in \Sigma_0$ ,  $R \in SO(3)$ ,  $D$  an elementary region in the  $xy$  plane,  $q$  a shape function of a surface parametrized by a function  $c$  from  $D$  into  $\mathbb{R}^3$ , then  $(Rq, h) = R(q, h)$ . That is, the actions on shape functions of homeomorphisms in  $\Sigma_0$  and matrices in  $SO(3)$  commute. For the sake of completeness we actually present the details of the justification of this fact in what follows. However, for this purpose, we first present a well-known formula about rotations and cross products of vectors in  $\mathbb{R}^3$  together

with its justification, again for the sake of completeness.

**Lemma:** Given vectors  $x, y$  in  $\mathbb{R}^3$ ,  $R$  in  $SO(3)$ , then  $R(x \times y) = Rx \times Ry$ .

**Proof:** Here given  $a, b, c$  in  $\mathbb{R}^3$ , we use the identity  $a \cdot (b \times c) = \det[a \ b \ c]$ , where  $\cdot$  and  $\det$  denote the inner product and determinant operations, respectively. In addition, for  $j = 1, 2, 3$ , we let  $e_j$  be the  $j^{\text{th}}$  unit vector in  $\mathbb{R}^3$ , and given  $w$  in  $\mathbb{R}^3$ , we let  $(w)_j$  denote the  $j^{\text{th}}$  coordinate of  $w$ . Since  $\det R = 1$  and  $RR^T$  equals the identity matrix, we then have for  $j = 1, 2, 3$ ,

$$\begin{aligned}
 (R(x \times y))_j &= e_j \cdot R(x \times y) = e_j^T R(x \times y) = (R^T e_j)^T (x \times y) \\
 &= R^T e_j \cdot (x \times y) = \det[R^T e_j \ x \ y] \\
 &= \det R \det[R^T e_j \ x \ y] = \det R [R^T e_j \ x \ y] \\
 &= \det[RR^T e_j \ Rx \ Ry] = \det[e_j \ Rx \ Ry] \\
 &= e_j \cdot (Rx \times Ry) = (Rx \times Ry)_j.
 \end{aligned}$$

Thus  $R(x \times y) = Rx \times Ry$ . □

With  $h, R, q, c$  as above, in order to show  $(Rq, h) = R(q, h)$ , we first show that the shape function of  $Rc$  on  $D$ , say  $\hat{q}$ , is  $Rq$ . From the definition of a shape function and the lemma then

$$\begin{aligned}
 \hat{q} &= \left( \frac{\partial Rc}{\partial u} \times \frac{\partial Rc}{\partial v} \right) / \sqrt{\left\| \frac{\partial Rc}{\partial u} \times \frac{\partial Rc}{\partial v} \right\|} = \left( R \frac{\partial c}{\partial u} \times R \frac{\partial c}{\partial v} \right) / \sqrt{\left\| R \frac{\partial c}{\partial u} \times R \frac{\partial c}{\partial v} \right\|} \\
 &= R \left( \frac{\partial c}{\partial u} \times \frac{\partial c}{\partial v} \right) / \sqrt{\left\| R \left( \frac{\partial c}{\partial u} \times \frac{\partial c}{\partial v} \right) \right\|} = R \left( \frac{\partial c}{\partial u} \times \frac{\partial c}{\partial v} \right) / \sqrt{\left\| \frac{\partial c}{\partial u} \times \frac{\partial c}{\partial v} \right\|} \\
 &= Rq.
 \end{aligned}$$

From Theorem 4 and what we just proved, it follows that the shape function of  $Rc(h)$  is then  $(Rq, h)$ . On the other hand, again by Theorem 4, the shape function of  $c(h)$  is  $(q, h)$  so that again by what we just proved the shape function of  $R(c(h))$  must be  $R(q, h)$ . Since  $Rc(h)$  and  $R(c(h))$  are the same function, then it must be that their shape functions are the same, i.e.,  $(Rq, h) = R(q, h)$ .

Based in part on the observations above about rotation matrices and homeomorphisms, in a manner similar to what is done in [6, 10], given  $S_1, S_2, c_1, c_2, q_1, q_2$  as above, with  $\inf$  short for infimum, it can be demonstrated that the number

$$\begin{aligned}
 &\inf_{R \in SO(3), h \in \Sigma_0} \|q_1 - R(q_2, h)\|_{2,D} = \\
 &\inf_{R \in SO(3), h \in \Sigma_0} \left( \int \int_D \|q_1 - R(q_2, h)\|^2 dr dt \right)^{1/2} =
 \end{aligned}$$



$$\inf_{R \in SO(3), h \in \Sigma_0} \left( \int \int_D \|q_1 - R(q_2 \circ h)\| \sqrt{\frac{\partial(u,v)}{\partial(r,t)}} \|^2 dr dt \right)^{1/2}$$

can be used as a well-defined distance between the surfaces  $S_1$  and  $S_2$ , where again  $\frac{\partial(u,v)}{\partial(r,t)}$  is the determinant of the Jacobian of  $h$ , and  $c_1$  and  $c_2$  are both normalized to parametrize surfaces of area equal to 1. Thus, denoting  $\inf_{R \in SO(3), h \in \Sigma_0} \|q_1 - R(q_2, h)\|_{2,D}$  by  $\text{dist}(S_1, S_2)$ , and restricting ourselves to the simpler region  $D = [0, 1] \times [0, 1]$ , then by Fubini's theorem, we note,

$$\begin{aligned} \text{dist}(S_1, S_2) &= \inf_{R \in SO(3), h \in \Sigma_0} \left( \int \int_D \|q_1 - R(q_2, h)\|^2 dr dt \right)^{1/2} \\ &= \inf_{R \in SO(3), h \in \Sigma_0} \left( \int_0^1 \int_0^1 \|q_1 - R(q_2, h)\|^2 dr dt \right)^{1/2} \end{aligned}$$

which we use in the next section.

## 5. Computation of Homeomorphism for Partial Registration of Surfaces using Dynamic Programming

In this section, ignoring rotations, we describe the computation, based on Dynamic Programming, of a homeomorphism for the partial elastic shape registration of two simple surfaces of unit area in 3-dimensional space. Given that  $S_1$  and  $S_2$  are the two surfaces, with  $D = [0, 1] \times [0, 1]$ , we assume accordingly that one-to-one functions  $c_1$  and  $c_2$  exist of class  $C^1$ ,  $c_1 : D \rightarrow \mathbb{R}^3$ ,  $c_2 : D \rightarrow \mathbb{R}^3$ , such that  $S_1 = c_1(D)$  and  $S_2 = c_2(D)$ . That is,  $c_1$  and  $c_2$  parametrize or are parametrizations of  $S_1$  and  $S_2$ , respectively. Given that  $q_1$  and  $q_2$  are, respectively, the shape functions of  $c_1$  and  $c_2$ , then we hope to minimize

$$\begin{aligned} \int \int_D \|q_1 - (q_2, h)\|^2 dr dt &= \int \int_D \|q_1 - (q_2 \circ h)\| \sqrt{\frac{\partial(u,v)}{\partial(r,t)}} \|^2 dr dt \\ &= \int_0^1 \int_0^1 \|q_1 - (q_2 \circ h)\| \sqrt{\frac{\partial(u,v)}{\partial(r,t)}} \|^2 dr dt \end{aligned}$$

with respect to  $h$  in  $\Sigma_0$ , where  $\Sigma_0$  is the set of all  $C^1$  homeomorphisms  $h$  from  $D$  onto itself, with  $\frac{\partial(u,v)}{\partial(r,t)} > 0$  on  $D$ ,  $\frac{\partial(u,v)}{\partial(r,t)}$  the determinant of the Jacobian of  $h$ . We note, this minimization is usually carried out with an algorithm that uses a gradient approach for the optimization over reparametrizations, i.e., over homeomorphisms  $h$  in  $\Sigma_0$ , that may produce a local solution [6, 10]. In this paper we have opted to carry out the minimization with respect to  $h$  in a special subset of  $\Sigma_0$  that allows for the use of Dynamic Programming. We denote this subset of  $\Sigma_0$  by  $\Sigma_1$ ,  $h$  in  $\Sigma_1$  satisfying that  $h \in \Sigma_0$  and for  $(r, t)$  in  $D$ , if  $h(r, t) = (\hat{r}, \hat{t})$  then it must be that  $\hat{t} = t$ . In addition, if  $h \in \Sigma_1$ , we assume for any  $t$  in  $[0, 1]$  that  $h(0, t) = (0, t)$  and  $h(1, t) = (1, t)$ . That a minimization over  $\Sigma_1$  allows for the use of Dynamic Programming will become evident below. Note, from Theorem 2, with  $\partial D$  the

boundary of  $D$ , for any homeomorphism  $h$  from  $D$  onto itself, not necessarily in  $\Sigma_0$  or  $\Sigma_1$ , it must be that  $h(\partial D) = \partial D$ .

Since in practice we can only work with a discretized version of the problem, for our purposes we assume the situation is as follows: for positive integers  $M, N$ , not necessarily equal, and partitions of  $[0, 1]$ ,  $\{r_i\}_{i=1}^M$ ,  $r_1 = 0 < r_2 < \dots < r_M = 1$ ,  $\{t_j\}_{j=1}^N$ ,  $t_1 = 0 < t_2 < \dots < t_N = 1$ , not necessarily uniform,  $c_1$  and  $c_2$  are given as lists of  $M \times N$  points in the surfaces  $S_1$  and  $S_2$ , respectively, the lists for  $c_1$  and  $c_2$  corresponding to  $c_1(r_i, t_j)$  and  $c_2(r_i, t_j)$ ,  $i = 1, \dots, M$ ,  $j = 1, \dots, N$ , respectively; for  $k = 1, 2$ , the list for  $c_k$  given in the following order:  $c_k(r_1, t_1), c_k(r_2, t_1), \dots, c_k(r_M, t_1), \dots, c_k(r_1, t_N), c_k(r_2, t_N), \dots, c_k(r_M, t_N)$ .

Computing  $\frac{\partial c_1}{\partial r}(r_i, t_j)$ ,  $\frac{\partial c_1}{\partial t}(r_i, t_j)$ ,  $\frac{\partial c_2}{\partial r}(r_i, t_j)$ ,  $\frac{\partial c_2}{\partial t}(r_i, t_j)$  with centered finite differences from  $c_1(r_i, t_j)$  and  $c_2(r_i, t_j)$ , for  $i = 1, \dots, M$ ,  $j = 1, \dots, N$ , we can then approximately compute for  $i = 1, \dots, M$ ,  $j = 1, \dots, N$ ,  $k = 1, 2$ ,

$$q_k(r_i, t_j) = \left( \left( \frac{\partial c_k}{\partial r} \times \frac{\partial c_k}{\partial t} \right) / \sqrt{\left\| \frac{\partial c_k}{\partial r} \times \frac{\partial c_k}{\partial t} \right\|} \right)(r_i, t_j),$$

(3-dimensional zero if  $(\frac{\partial c_k}{\partial r} \times \frac{\partial c_k}{\partial t})(r_i, t_j)$  equals 3-dimensional zero).

Finally we note that if  $h \in \Sigma_1$ , then  $h(r, t) = (u(r, t), v(r, t)) = (u(r, t), t)$  for  $(r, t)$  in  $D$ , so that  $\frac{\partial v}{\partial r}(r, t) = 0$  and  $\frac{\partial v}{\partial t}(r, t) = 1$ , and therefore  $\frac{\partial(u, v)}{\partial(r, t)}(r, t) = \frac{\partial u}{\partial r}(r, t)$  for  $(r, t)$  in  $D$ .

Given  $h$  in  $\Sigma_1$  and an integer  $j$ ,  $1 \leq j \leq N$ , next we discretize the integral

$$\int_0^1 \left\| q_1(r, t_j) - \left( (q_2 \circ h) \sqrt{\frac{\partial(u, v)}{\partial(r, t)}} \right)(r, t_j) \right\|^2 dr.$$

For this purpose, we define  $q_{1j}(r_i)$ ,  $q_{2j}(r_i)$  in  $\mathbb{R}^3$  for  $i = 1, \dots, M$ , by

$$q_{1j}(r_i) = q_1(r_i, t_j), \quad q_{2j}(r_i) = q_2(r_i, t_j),$$

and define as well a diffeomorphism  $h_j$  from  $[0, 1]$  onto  $[0, 1]$  by

$$h_j(r) = u(r, t_j), \quad r \in [0, 1].$$

Note,  $h_j$  is indeed a diffeomorphism as clearly  $h_j(0) = 0$ ,  $h_j(1) = 1$ , and for  $r \in [0, 1]$ ,  $h'_j(r) = \frac{dh_j}{dr}(r) = \frac{\partial u}{\partial r}(r, t_j) = \frac{\partial(u, v)}{\partial(r, t)}(r, t_j) > 0$ .

For  $i = 1, \dots, M$ , we can then compute  $h_j(r_i) = u(r_i, t_j)$  so that  $h_j(r_1) = h_j(0) = 0$  and  $h_j(r_M) = h_j(1) = 1$ . In addition, for  $i = 1, \dots, M-1$ , we compute  $\Delta r_i = r_{i+1} - r_i$ , approximately compute  $h'_j(r_i) = (h_j(r_{i+1}) - h_j(r_i)) / \Delta r_i$ , set  $h'_j(r_M) = h'_j(r_1)$ , and by interpolating  $q_{2j}(r_i)$ ,  $i = 1, \dots, M$ , by a cubic spline, for  $i = 1, \dots, M$ , we can approximately compute  $q_{2j}(h_j(r_i))$ , which in turn is an approximation of  $(q_2 \circ h)(r_i, t_j)$  as  $(q_2 \circ h)(r_i, t_j) =$

$q_2(h(r_i, t_j)) = q_2(u(r_i, t_j), t_j) = q_2(h_j(r_i), t_j) = q_{2j}(h_j(r_i))$  if  $q_{2j}(r)$  is interpreted to be  $q_2(r, t_j)$  for every  $r \in [0, 1]$ . Thus, with the trapezoidal rule the integral is discretized by

$$E(h_j) = \frac{1}{2} \sum_{i=1}^{M-1} \Delta r_i (E_{i+1}^j + E_i^j)$$

where for  $i = 1, \dots, M$ ,

$$E_i^j = \|q_{1j}(r_i) - q_{2j}(h_j(r_i))\sqrt{h'_j(r_i)}\|^2.$$

From this, again using the trapezoidal rule, we can then discretize the double integral

$$\int_0^1 \int_0^1 \|q_1(r, t) - ((q_2 \circ h) \sqrt{\frac{\partial(u, v)}{\partial(r, t)}})(r, t)\|^2 dr dt$$

by

$$E = \frac{1}{2} \sum_{j=1}^{N-1} \Delta t_j (E(h_{j+1}) + E(h_j)),$$

where for  $j = 1, \dots, N-1$ ,  $\Delta t_j = t_{j+1} - t_j$ .

Given  $j$ ,  $1 \leq j \leq N$ , treating now  $h_j(r_i)$ ,  $i = 1, \dots, M$ , in the definition of  $E(h_j)$  as the discretization of any diffeomorphism  $h_j$  from  $[0, 1]$  onto  $[0, 1]$ , if for each  $j$ ,  $j = 1, \dots, N$ , we can find  $h_j$  whose discretization minimizes  $E(h_j)$ , then the collection of diffeomorphisms  $h_j$ ,  $j = 1, \dots, N$ , minimizes  $E$ , and a homeomorphism  $h$  in  $\Sigma_1$  can be identified such that  $h(r_i, t_j) = (h_j(r_i), t_j)$ ,  $i = 1, \dots, M$ ,  $j = 1, \dots, N$ . Thus, the double integral above is approximately minimized by  $h$  among all homeomorphisms in  $\Sigma_1$ , with the value of the double integral approximately equal to  $E$ .

In [4], algorithm *adapt-DP*, an algorithm based on Dynamic Programming, was presented for approximately computing, ignoring rotations, the elastic shape registration of two curves in  $d$ -dimensional space. The algorithm was originally presented in [1] for  $d = 2$ . Given that  $\hat{q}_1$  and  $\hat{q}_2$  are discretizations of the shape functions of the two curves,  $\hat{q}_1$  and  $\hat{q}_2$  are used as input for algorithm *adapt-DP* to compute a discretization of a diffeomorphism for reparametrizing the second curve, the reparametrization then resulting in an approximate elastic shape registration of the two curves. Even though for  $j = 1, \dots, N$ ,  $q_{1j}$  and  $q_{2j}$  as defined above are not exactly computed as discretizations of the shape functions of curves in 3-dimensional space, with algorithm *adapt-DP* for  $d = 3$  with  $q_{1j}$ ,  $q_{2j}$  taking the place of  $\hat{q}_1$ ,  $\hat{q}_2$ , respectively, we can still compute the discretization of some diffeomorphism  $h_j$ , i.e.,  $h_j(r_i)$ ,  $i = 1, \dots, M$ , that approximately minimizes  $E(h_j)$ . Having done this for each  $j$ ,  $j = 1, \dots, N$ ,  $h$  in  $\Sigma_1$  can then be identified such that  $h(r_i, t_j) = (h_j(r_i), t_j)$ ,  $i = 1, \dots, M$ ,  $j = 1, \dots, N$ , and, ignoring rotations,  $c_1$ ,  $c_2(h)$  are interpreted to achieve

approximately the partial elastic shape registration of the two surfaces. Computing  $E = \frac{1}{2} \sum_{j=1}^{N-1} \Delta t_j (E(h_{j+1}) + E(h_j))$ , again ignoring rotations, then  $\sqrt{E}$  is interpreted to be approximately the elastic shape distance between the two surfaces corresponding to the partial elastic shape registration of the two surfaces.

## 6. Computation of Rotation Matrix for Rigid Alignment of Surfaces

In this section, we describe the computation of an approximately optimal rotation matrix for the rigid alignment of two simple surfaces of unit area in 3–dimensional space. Given that  $S_1$  and  $S_2$  are the two surfaces, with  $D$ ,  $c_1$ ,  $c_2$ ,  $q_1$ ,  $q_2$  as in the previous section, we hope to minimize

$$\int \int_D \|q_1(r,t) - Rq_2(r,t)\|^2 dr dt = \int_0^1 \int_0^1 \|q_1(r,t) - Rq_2(r,t)\|^2 dr dt$$

with respect to rotation matrices  $R$  in 3–dimensional space, i.e., with respect to  $3 \times 3$  matrices  $R$  that are orthogonal and have determinant equal to 1, i.e., with respect to matrices  $R$  in  $SO(3)$ .

As in the previous section, we must work with a discretized version of the problem. Thus we assume again that for positive integers  $M$ ,  $N$ , not necessarily equal, and partitions of  $[0, 1]$ ,  $\{r_i\}_{i=1}^M$ ,  $r_1 = 0 < r_2 < \dots < r_M = 1$ ,  $\{t_j\}_{j=1}^N$ ,  $t_1 = 0 < t_2 < \dots < t_N = 1$ , not necessarily uniform,  $c_1$  and  $c_2$  are given as lists of  $M \times N$  points in the surfaces  $S_1$  and  $S_2$ , respectively, the lists for  $c_1$  and  $c_2$  corresponding to  $c_1(r_i, t_j)$  and  $c_2(r_i, t_j)$ ,  $i = 1, \dots, M$ ,  $j = 1, \dots, N$ , respectively, and that  $q_1(r_i, t_j)$  and  $q_2(r_i, t_j)$  are approximately computed from  $c_1(r_i, t_j)$  and  $c_2(r_i, t_j)$ ,  $i = 1, \dots, M$ ,  $j = 1, \dots, N$ , as in the previous section. With  $\Delta r_i = r_{i+1} - r_i$ ,  $i = 1, \dots, M-1$ , for  $R$  in  $SO(3)$ , and an integer  $j$ ,  $1 \leq j \leq N$ , next with the trapezoidal rule we discretize the integral

$$\int_0^1 \|q_1(r, t_j) - Rq_2(r, t_j)\|^2 dr$$

by

$$\begin{aligned} F_j &= \frac{1}{2} \sum_{i=1}^{M-1} \Delta r_i (\|q_1(r_i, t_j) - Rq_2(r_i, t_j)\|^2 + \|q_1(r_{i+1}, t_j) - Rq_2(r_{i+1}, t_j)\|^2) \\ &= \sum_{i=1}^M \Delta \tilde{r}_i \|q_1(r_i, t_j) - Rq_2(r_i, t_j)\|^2, \end{aligned}$$

where  $\Delta \tilde{r}_1 = (r_2 - r_1)/2$ ,  $\Delta \tilde{r}_M = (r_M - r_{M-1})/2$ , and for  $i = 2, \dots, M-1$ ,  $\Delta \tilde{r}_i = (r_{i+1} - r_{i-1})/2$ . Note,  $\Delta \tilde{r}_i > 0$  for  $i = 1, \dots, M$ , and  $\sum_{i=1}^M \Delta \tilde{r}_i = 1$ .

From this, with  $\Delta t_j = t_{j+1} - t_j$ ,  $j = 1, \dots, N-1$ , again using the trapezoidal rule and noting

that  $\|Rq_2(r_i, t_j)\| = \|q_2(r_i, t_j)\|$ ,  $i = 1, \dots, M$ ,  $j = 1, \dots, N$ , we can then discretize the double integral

$$\int_0^1 \int_0^1 \|q_1(r, t) - Rq_2(r, t)\|^2 dr dt$$

by

$$\begin{aligned} F &= \frac{1}{2} \sum_{j=1}^{N-1} \Delta t_j (F_{j+1} + F_j) = \sum_{j=1}^N \Delta \tilde{t}_j F_j \\ &= \sum_{j=1}^N \Delta \tilde{t}_j \left( \sum_{i=1}^M \Delta \tilde{r}_i \|q_1(r_i, t_j) - Rq_2(r_i, t_j)\|^2 \right) \\ &= \sum_{j=1}^N \Delta \tilde{t}_j \left( \sum_{i=1}^M \Delta \tilde{r}_i (\|q_1(r_i, t_j)\|^2 + \|q_2(r_i, t_j)\|^2) \right) \\ &\quad - 2 \sum_{j=1}^N \Delta \tilde{t}_j \left( \sum_{i=1}^M \Delta \tilde{r}_i ((q_1(r_i, t_j))^T Rq_2(r_i, t_j)) \right), \end{aligned}$$

where  $\Delta \tilde{t}_1 = (t_2 - t_1)/2$ ,  $\Delta \tilde{t}_N = (t_N - t_{N-1})/2$ , and for  $j = 2, \dots, N-1$ ,  $\Delta \tilde{t}_j = (t_{j+1} - t_{j-1})/2$ . Note,  $\Delta \tilde{t}_j > 0$  for  $j = 1, \dots, N$ , and  $\sum_{j=1}^N \Delta \tilde{t}_j = 1$ .

Thus, minimizing  $F$  over all rotations  $R$  in  $SO(3)$  is equivalent to maximizing over the same set of rotations

$$\sum_{j=1}^N \Delta \tilde{t}_j \left( \sum_{i=1}^M \Delta \tilde{r}_i ((q_1(r_i, t_j))^T Rq_2(r_i, t_j)) \right) = \text{tr}(RA^T),$$

where  $A$  is the  $3 \times 3$  matrix with entries

$$A_{kl} = \sum_{j=1}^N \Delta \tilde{t}_j \left( \sum_{i=1}^M \Delta \tilde{r}_i (q_1(r_i, t_j)_k q_2(r_i, t_j)_l) \right),$$

for each pair  $k, l = 1, 2, 3$ ,  $q_1(r_i, t_j)_k$  the  $k^{\text{th}}$  coordinate of  $q_1(r_i, t_j)$ , and  $q_2(r_i, t_j)_l$  the  $l^{\text{th}}$  coordinate of  $q_2(r_i, t_j)$ ,  $i = 1, \dots, M$ ,  $j = 1, \dots, N$ , and  $\text{tr}(RA^T)$  is the trace of the matrix  $RA^T$ .

Accordingly, an optimal rotation matrix  $R$  for maximizing  $\text{tr}(RA^T)$  can be computed from the singular value decomposition of  $A$  or, more precisely, with the Kabsch-Umeyama algorithm [3, 8, 9, 11, 16] (see Algorithm Kabsch-Umeyama below for 3-dimensional surfaces, where  $\text{diag}\{s_1, s_2, s_3\}$  is the  $3 \times 3$  diagonal matrix with numbers  $s_1, s_2, s_3$  as the elements of the diagonal, in that order running from the upper left to the lower right of the matrix). A *singular value decomposition* (SVD) [12] of  $A$  is a representation of the form  $A = USV^T$ , where  $U$  and  $V$  are  $3 \times 3$  orthogonal matrices and  $S$  is a  $3 \times 3$  diagonal matrix with the singular values of  $A$ , which are nonnegative real numbers, appearing in the diagonal of  $S$  in descending order, from the upper left to the lower right

of  $S$ . Finally, note that the SVD concept can be generalized so that any matrix of any dimension, not necessarily square, has a singular value decomposition, not necessarily unique [12].

---

**Algorithm Kabsch-Umeyama** for surfaces (KU3 algorithm)

---

Set  $\Delta\tilde{r}_1 = (r_2 - r_1)/2$ ,  $\Delta\tilde{r}_M = (r_M - r_{M-1})/2$ , and for  $i = 2, \dots, M-1$ ,  $\Delta\tilde{r}_i = (r_{i+1} - r_{i-1})/2$ .

Set  $\Delta\tilde{t}_1 = (t_2 - t_1)/2$ ,  $\Delta\tilde{t}_N = (t_N - t_{N-1})/2$ , and for  $j = 2, \dots, N-1$ ,  $\Delta\tilde{t}_j = (t_{j+1} - t_{j-1})/2$ .

Set  $q_1(r_i, t_j)_k$  equal to the  $k^{\text{th}}$  coordinate of  $q_1(r_i, t_j)$  for  $i = 1, \dots, M$ ,  $j = 1, \dots, N$ ,  $k = 1, 2, 3$ .

Set  $q_2(r_i, t_j)_l$  equal to the  $l^{\text{th}}$  coordinate of  $q_2(r_i, t_j)$  for  $i = 1, \dots, M$ ,  $j = 1, \dots, N$ ,  $l = 1, 2, 3$ .

Compute  $A_{kl} = \sum_{j=1}^N \Delta\tilde{t}_j (\sum_{i=1}^M \Delta\tilde{r}_i (q_1(r_i, t_j)_k q_2(r_i, t_j)_l))$

for each pair  $k, l = 1, 2, 3$ .

Identify  $3 \times 3$  matrix  $A$  with entries  $A_{kl}$  for each pair  $k, l = 1, 2, 3$ .

Compute SVD of  $A$ , i.e., identify  $3 \times 3$  matrices  $U, S, V$ , so that

$A = USV^T$  in the SVD sense.

Set  $s_1 = s_2 = 1$ .

**if**  $\det(UV) > 0$  **then** set  $s_3 = 1$ .

**else** set  $s_3 = -1$ . **end if**

Set  $\tilde{S} = \text{diag}\{s_1, s_2, s_3\}$ .

Compute and return  $R = U\tilde{S}V^T$  and  $\text{maxtrace} = \text{tr}(RA^T)$ .

---

## 7. Procedure for Optimizing over both Rotations and Reparametrizations using Dynamic Programming

With  $D = [0, 1] \times [0, 1]$ ,  $c_1, c_2, q_1, q_2, S_1, S_2$  as above,  $R$  in  $SO(3)$ ,  $h$  in  $\Sigma_0$ , so that  $\frac{\partial(u,v)}{\partial(r,t)}$ , the determinant of the Jacobian of  $h$ , is positive on  $D$ , we hope to minimize

$$\int_0^1 \int_0^1 \|q_1(r,t) - (R(q_2 \circ h) \sqrt{\frac{\partial(u,v)}{\partial(r,t)}})(r,t)\|^2 dr dt$$

with respect to  $R$  and  $h$ .

We note, using arguments as those in [5], the above minimization problem can be reformulated as that of minimizing

$$\int_0^1 \int_0^1 \|Rq_1(r,t) - ((q_2 \circ h) \sqrt{\frac{\partial(u,v)}{\partial(r,t)}})(r,t)\|^2 dr dt$$

with respect to  $R$  and  $h$ .

This allows for the second surface to be reparametrized while the first one is rotated. Of course, as already noted above, we work with  $\Sigma_1$ , as defined above, instead of  $\Sigma_0$  of which it is a subset, as this allows for the use of Dynamic Programming when optimizing over reparametrizations of the second surface. Assuming  $M, N, r_i, i = 1, \dots, M, t_j, j = 1, \dots, N, c_1(r_i, t_j), c_2(r_i, t_j), q_1(r_i, t_j), q_2(r_i, t_j), i = 1, \dots, M, j = 1, \dots, N$ , are as in the previous sections, for the purpose of approximately minimizing the second double integral above with respect to  $R$  in  $SO(3)$ ,  $h$  in  $\Sigma_1$ , we use the procedure below that alternates computations of discretizations of approximately optimal homeomorphisms in  $\Sigma_1$  using Dynamic Programming (one per iteration for reparametrizing the second surface) and approximately optimal rotation matrices (one per iteration for rotating the first surface), these computations as described in the previous two sections. The procedure, Procedure DP-surface-min, with  $c_1(r_i, t_j), c_2(r_i, t_j), q_1(r_i, t_j), q_2(r_i, t_j), i = 1, \dots, M, j = 1, \dots, N$ , as input, is summarized below. In it, given discretizations  $q(r_i), \hat{q}(r_i), i = 1, \dots, M$ , of functions  $q, \hat{q}$ , treated as discretizations of shape functions of curves in 3-dimensional space, to say “Execute DP algorithm for  $q(r_i), \hat{q}(r_i), i = 1, \dots, M$ ” will mean the DP algorithm (*adapt-DP* for  $d = 3$ ) should be executed with  $q(r_i), \hat{q}(r_i), i = 1, \dots, M$ , as input, as described in Section 5 above. Also, given  $\tilde{q}_1(r_i, t_j), \tilde{q}_2(r_i, t_j), i = 1, \dots, M, j = 1, \dots, N$ , discretizations of shape functions  $\tilde{q}_1, \tilde{q}_2$  of the two surfaces, to say “Execute KU3 algorithm for  $\tilde{q}_1(r_i, t_j), \tilde{q}_2(r_i, t_j), i = 1, \dots, M, j = 1, \dots, N$ ” will mean the Kabsch-Umeyama algorithm for surfaces, outlined in the previous section, should be executed with  $\tilde{q}_1, \tilde{q}_2$  taking the place of  $q_1, q_2$ , respectively, in the algorithm.

---

### Procedure DP-surface-min

---

Set  $\Delta r_i = r_{i+1} - r_i, i = 1, \dots, M - 1$ .

Set  $\Delta \tilde{r}_1 = (r_2 - r_1)/2, \Delta \tilde{r}_M = (r_M - r_{M-1})/2$ , and for  $i = 2, \dots, M - 1, \Delta \tilde{r}_i = (r_{i+1} - r_{i-1})/2$ .

Set  $\Delta \tilde{t}_1 = (t_2 - t_1)/2, \Delta \tilde{t}_N = (t_N - t_{N-1})/2$ , and for  $j = 2, \dots, N - 1, \Delta \tilde{t}_j = (t_{j+1} - t_{j-1})/2$ .

Set  $\hat{q}_2(r_i, t_j) = q_2(r_i, t_j)$  for  $i = 1, \dots, M, j = 1, \dots, N$ .

Set  $iter = 0, E^{curr} = 10^6, iten = 10, tol = 10^{-6}$ .

**repeat**

    Set  $iter = iter + 1, E^{prev} = E^{curr}$ .

    Execute KU3 algorithm for  $\hat{q}_2(r_i, t_j), q_1(r_i, t_j), i = 1, \dots, M, j = 1, \dots, N$ , to get rotation matrix  $R$ .

    Set  $\hat{q}_1(r_i, t_j) = Rq_1(r_i, t_j)$  for  $i = 1, \dots, M, j = 1, \dots, N$ .

**for**  $j = 1, \dots, N$  **do**

        Set  $q_{1j}(r_i) = \hat{q}_1(r_i, t_j), q_{2j}(r_i) = q_2(r_i, t_j), i = 1, \dots, M$ .

        Execute DP algorithm for  $q_{1j}(r_i), q_{2j}(r_i), i = 1, \dots, M$ , to get discretization of diffeomorphism  $h_j: h_j(r_i), i = 1, \dots, M$ .

        Set  $h'_j(r_i) = (h_j(r_{i+1}) - h_j(r_i))/\Delta r_i$  for  $i = 1, \dots, M - 1$ ,

$h'_j(r_M) = h'_j(r_1)$ .  
 From interpolation of  $q_{2j}(r_i)$ ,  $i = 1, \dots, M$ , with a cubic spline  
 set  $\hat{q}_{2j}(r_i) = \sqrt{h'_j(r_i)q_{2j}(h_j(r_i))}$  for  $i = 1, \dots, M$ .  
 Compute  $E(h_j) = \sum_{i=1}^M \Delta \tilde{r}_i \|q_{1j}(r_i) - \sqrt{h'_j(r_i)q_{2j}(h_j(r_i))}\|^2$   
 $= \sum_{i=1}^M \Delta \tilde{r}_i \|q_{1j}(r_i) - \hat{q}_{2j}(r_i)\|^2$ .  
 Set  $\hat{q}_2(r_i, t_j) = \hat{q}_{2j}(r_i)$  for  $i = 1, \dots, M$ .  
**end for**  
 $E^{curr} = \sum_{j=1}^N \Delta \tilde{t}_j E(h_j)$ .  
**until**  $|E^{curr} - E^{prev}| < tol$  or  $iter > iten$ .  
 $E = E^{curr}$ .  
**for**  $j = 1, \dots, N$  **do**  
 Set  $h(r_i, t_j) = (h_j(r_i), t_j)$  for  $i = 1, \dots, M$ .  
 Set  $c_{2j}(r_i) = c_2(r_i, t_j)$  for  $i = 1, \dots, M$ .  
 From interpolation of  $c_{2j}(r_i)$ ,  $i = 1, \dots, M$ , with a cubic spline  
 set  $\hat{c}_2(r_i, t_j) = c_{2j}(h_j(r_i))$  for  $i = 1, \dots, M$ .  
**end for**  
 Set  $\hat{c}_1(r_i, t_j) = Rc_1(r_i, t_j)$  for  $i = 1, \dots, M$ ,  $j = 1, \dots, N$ .  
 Return  $E$ ,  $R$ ,  $h(r_i, t_j)$ ,  $\hat{c}_1(r_i, t_j)$ ,  $\hat{q}_1(r_i, t_j)$ ,  $\hat{c}_2(r_i, t_j)$ ,  $\hat{q}_2(r_i, t_j)$ ,  
 $i = 1, \dots, M$ ,  $j = 1, \dots, N$ .

---

On output, restricting ourselves to homeomorphisms in  $\Sigma_1$ ,  $E$  is interpreted to be the square of the elastic shape distance between  $c_1$  and  $c_2$ ;  $\hat{c}_1(r_i, t_j)$  and  $\hat{c}_2(r_i, t_j)$ ,  $i = 1, \dots, M$ ,  $j = 1, \dots, N$ , are interpreted to achieve the elastic shape registration of  $c_1$  and  $c_2$ ;  $\hat{q}_1$  and  $\hat{q}_2$  are the shape functions of  $\hat{c}_1$  and  $\hat{c}_2$ , respectively;  $R$  is the optimal rotation matrix and  $h$  is the optimal homeomorphism in  $\Sigma_1$  with which everything is computed. Everything including  $R$  and  $h$  approximately computed.

## 8. Results from Implementation of Methods

A software package that incorporates the methods presented in this paper for computing, using Dynamic Programming, a partial elastic shape registration of two simple surfaces in 3-dimensional space, and therefore the elastic shape distance between them associated with this partial registration, has been implemented. The implementation is in Matlab<sup>1</sup> with the exception of the Dynamic Programming routine which is written in Fortran but is executed as a Matlab mex file. In this section, we present results obtained from executions of the software package. We note, the software package as well as input data files, a README file, etc. can be obtained at the following link

<https://doi.org/10.18434/mds2-3056>

---

<sup>1</sup>The identification of any commercial product or trade name does not imply endorsement or recommendation by the National Institute of Standards and Technology.



We note, Matlab file ESD\_driv\_surf\_3d.m is the driver routine of the package, and Fortran routine DP\_MEX\_WNDSTRP\_ALLDIM.F is the Dynamic Programming routine which has already been processed (with parameter dimx = 3) to be executed as a Matlab mex file. In case the Fortran routine must be processed to obtain a new mex file, this can be done by typing in the Matlab window:

```
mex -compatibleArrayDims DP_MEX_WNDSTRP_ALLDIM.F
```

At the start of the execution of the software, we assume  $S_1, S_2$  are the two simple surfaces in 3-dimensional space under consideration, with functions  $c_1, c_2 : D \equiv [0, T_1] \times [0, T_2] \rightarrow \mathbb{R}^3$ ,  $T_1, T_2 > 0$ , as their parametrizations, respectively, so that  $S_1 = c_1(D)$ ,  $S_2 = c_2(D)$ . We also assume that as input to the software, for positive integers  $M, N$ , not necessarily equal, and partitions of  $[0, T_1]$ ,  $[0, T_2]$ , respectively,  $\{r_i\}_{i=1}^M$ ,  $r_1 = 0 < r_2 < \dots < r_M = T_1$ ,  $\{t_j\}_{j=1}^N$ ,  $t_1 = 0 < t_2 < \dots < t_N = T_2$ , not necessarily uniform, discretizations of  $c_1, c_2$  are given, each discretization in the form of a list of  $M \times N$  points in the corresponding surface, namely  $c_1(r_i, t_j)$  and  $c_2(r_i, t_j)$ ,  $i = 1, \dots, M$ ,  $j = 1, \dots, N$ , respectively, and for  $k = 1, 2$ , as specified in the Introduction section, in the order  $c_k(r_1, t_1), c_k(r_2, t_1), \dots, c_k(r_M, t_1), \dots, c_k(r_1, t_N), c_k(r_2, t_N), \dots, c_k(r_M, t_N)$ . Based on this input, for the purpose of computing, using Dynamic Programming, a partial elastic shape registration of  $S_1$  and  $S_2$ , together with the elastic shape distance between them associated with the partial registration, the program always proceeds first to scale the partitions  $\{r_i\}_{i=1}^M, \{t_j\}_{j=1}^N$ , so that they become partitions of  $[0, 1]$ , and to compute an approximation of the area of each surface. During the execution of the software package, the former is accomplished by Matlab routine ESD\_driv\_surf\_3d.m, while the latter by Matlab routine ESD\_comp\_surf\_3d.m through the computation for each  $k$ ,  $k = 1, 2$  of the sum of the areas of triangles with vertices  $c_k(r_i, t_j), c_k(r_{i+1}, t_{j+1}), c_k(r_i, t_{j+1})$ , and  $c_k(r_i, t_j), c_k(r_{i+1}, t_j), c_k(r_{i+1}, t_{j+1})$ , for  $i = 1, \dots, M - 1, j = 1, \dots, N - 1$ . The program then proceeds to scale the discretizations of the parametrizations of the two surfaces so that each surface has approximate area equal to 1 (given a surface and its approximate area, each point in the discretization of the parametrization of the surface is divided by the square root of half the approximate area of the surface). Once routine ESD\_comp\_surf\_3d.m is done, the actual computations of the partial registration and associated elastic shape distance are carried out by Matlab routine ESD\_core\_surf\_3d.m in which the methods for this purpose presented in this paper, mainly Procedure DP-surface-min in Section 7, have been implemented.

The results that follow were obtained from applications of our software package on discretizations of three kinds of surfaces in 3-dimensional space that we call surfaces of the sine, helicoid and cosine-sine kind. On input all surfaces were given as discretizations on the unit square  $([0, 1] \times [0, 1])$ , each interval  $[0, 1]$  uniformly partitioned into 100 intervals so that the unit square was thus partitioned into 10000 squares, each square of size  $0.01 \times 0.01$ , their corners making up a set of 10201 points. Using the notation used at the beginning of this section, the uniform partitions of the two  $[0, 1]$  intervals that define the unit square were then  $\{r_i\}_{i=1}^M, \{t_j\}_{j=1}^N$ , with  $M = N = 101$ ,  $r_{101} = t_{101} = 1.0$ , thus already scaled from the

start as required, and by evaluating the surfaces at the 10201 points identified above in the order as specified above and in the Introduction section, a discretization of each surface was obtained consisting of 10201 points. Given a pair of surfaces of one of the three kinds mentioned above, and given that a partial elastic shape registration of the two surfaces and the elastic shape distance between them associated with the partial registration were to be computed, one surface was identified as the first surface, the other one as the second surface (in the procedure for optimizing over rotations and reparametrizations using Dynamic Programming as described in Section 7, Procedure DP-surface-min, the second surface is reparametrized while the first one is rotated). For the purpose of testing the capability of the software for optimizing over reparametrizations based on Dynamic Programming, again using the notation used at the beginning of this section, for  $\gamma$ , a bijective function on the unit square to be defined below, with  $(\hat{r}_i, \hat{t}_j) = \gamma(r_i, t_j)$ ,  $i = 1, \dots, 101$ ,  $j = 1, \dots, 101$ , the second surface was reparametrized through its discretization, namely by setting  $\hat{c}_2 = c_2$  and computing  $c_2(r_i, t_j) = \hat{c}_2(\hat{r}_i, \hat{t}_j)$ ,  $i = 1, \dots, 101$ ,  $j = 1, \dots, 101$ , while the first surface was kept as originally defined and discretized by computing  $c_1(r_i, t_j)$ ,  $i = 1, \dots, 101$ ,  $j = 1, \dots, 101$ . Given the pair of surfaces, the program then, using the discretizations of the surfaces as just described in terms of  $c_1$ ,  $c_2$ , etc., after computing an approximation of the area of each surface and scaling each surface to have approximate area equal to 1, proceeded to compute a partial elastic shape registration of the two surfaces and the elastic shape distance between them associated with the partial registration. We note that because  $N$  equaled 101, during the execution the software package, the Dynamic Programming software was executed 101 times each time the **repeat** loop in Procedure DP-surface-min was executed. Finally, we note again that in what follows we refer to homeomorphisms on  $[0, 1]$  as diffeomorphisms in order to distinguish them from homeomorphisms on the unit square in the plane.

The first results that follow were obtained from applications of our software package on discretizations of surfaces in 3-dimensional space that are actually graphs of 3-dimensional functions based on the sine curve. Given  $k$ , a positive integer, one type of surface to which we refer as a surface of the sine kind (type 1) is defined by

$$x(r, t) = r, \quad y(r, t) = t, \quad z(r, t) = \sin k\pi r, \quad (r, t) \in [0, 1] \times [0, 1],$$

and another one (type 2) by

$$x(r, t) = \sin k\pi r, \quad y(r, t) = r, \quad z(r, t) = t, \quad (r, t) \in [0, 1] \times [0, 1],$$

the former a rotation of the latter by applying the rotation matrix  $\begin{pmatrix} 0 & 1 & 0 \\ 0 & 0 & 1 \\ 1 & 0 & 0 \end{pmatrix}$  on the latter, thus of similar shape.

Three plots depicting surfaces (actually their boundaries) of the sine kind for different values of  $k$  are shown in Figure 2. (Note that in the plots there, the  $x$ -,  $y$ -,  $z$ - axes are not always to scale relative to one another). In each plot two surfaces of the sine kind appear. The two surfaces in the leftmost plot being of similar shape, clearly the elastic shape

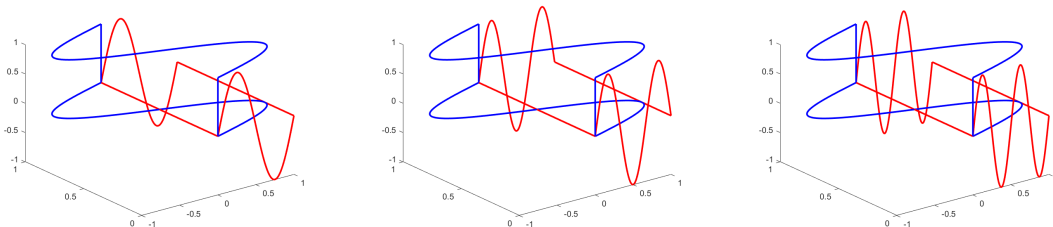


**Fig. 2.** Three plots of boundaries of surfaces of the sine kind. A partial elastic shape registration of the two surfaces in each plot and the elastic shape distance between them associated with the registration were computed.

distance between them is exactly zero, and the hope was then that the execution of our software package applied on these two surfaces would produce an elastic shape distance between them equal or close to zero. The type 2 surface in each plot (in blue) was considered to be the first surface in the plot. In each plot this surface was obtained by setting  $k$  equal to 2 in the definition above of a type 2 surface of the sine kind so that it is the same surface in all three plots. The other surface in each plot (in red) is a type 1 surface of the sine kind and was considered to be the second surface in each plot. From left to right in the three plots, the second surface was obtained by setting  $k$  equal to 2, 3, 4, respectively, in the definition above of a type 1 surface of the sine kind. As already mentioned above, in the procedure for optimizing over rotations and reparametrizations using Dynamic Programming as described in Section 7, Procedure DP-surface-min, the second surface is reparametrized while the first one is rotated.

With  $\gamma(r,t) = (r^{5/4}, t)$ ,  $(r,t) \in [0,1] \times [0,1]$ , all surfaces in the plots were then discretized as described above and a partial elastic shape registration of the two surfaces in each plot and the elastic shape distance between them associated with the partial registration were then computed through executions of our software package. We note that for this particular  $\gamma$ , the discretization of the second surface was perturbed only in the  $r$  direction which made the software package more likely to succeed as Procedure DP-surface-min always reparametrizes the second surface by applying the Dynamic Programming software exclusively on curves in 3-dimensional space contained in the surfaces in the  $r$  direction. The three elastic shape distances, computed in the order of the plots from left to right, were as follows with the first distance, as hoped for, essentially equal to zero: 0.0003 0.3479 0.3192. The times of execution in the same order were 27, 28, 39 seconds, with the **repeat** loop in Procedure DP-surface-min in Section 7 executed 3, 3, 4 times, respectively. The computed optimal rotation matrix for the pair of surfaces in the leftmost plot in Figure 2, was  $\begin{pmatrix} 0 & 1 & 0 \\ 0 & 0 & 1 \\ 1 & 0 & 0 \end{pmatrix}$ . For the other two pairs of surfaces the computed optimal rotation matrices were both almost equal to  $\begin{pmatrix} 0 & 1 & 0 \\ 0 & 0 & 1 \\ 1 & 0 & 0 \end{pmatrix}$  as well, their entries slightly different. It should be pointed out that because of the simplicity of surfaces of the sine kind and the

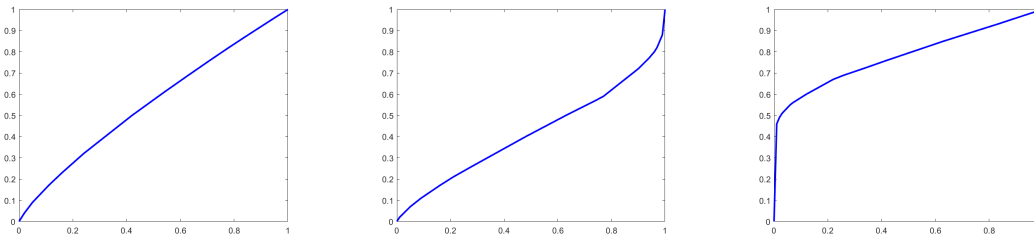


**Fig. 3.** Graphs of optimal diffeomorphisms from execution of Dynamic Programming software on the three pairs of surfaces with  $\gamma(r,t) = (r^{5/4}, t)$ ,  $(r,t) \in [0,1] \times [0,1]$ . One per pair, as for each pair the same two curves in 3–d space were used as input to the software each time it was executed. Thus the same diffeomorphism was computed each time for each pair of surfaces.

fact that for the given  $\gamma$  the discretization of the second surface was perturbed only in the  $r$  direction, whenever the Dynamic Programming software was executed for a given pair of surfaces, the same two curves in 3–dimensional space contained in the surfaces in the  $r$  direction were always used as input to the software. Therefore for the given pair, the same solution was obtained each time (101 times) the Dynamic Programming software was executed, in particular the same optimal orientation-preserving diffeomorphism from  $[0,1]$  onto  $[0,1]$  was computed each time together with the same elastic shape distance between the two curves in 3–dimensional space used as input to the software. Graphs of the optimal diffeomorphisms for each pair of surfaces in the order of the plots from left to right in Figure 2, are shown in Figure 3. In addition, Figure 4 shows results of the partial elastic shape registration of the pair of surfaces in the rightmost plot in Figure 2. The pair of surfaces is shown in the leftmost plot of the figure before any computations took place. In the middle plot we see the first surface after it was rotated with the corresponding computed optimal rotation matrix mentioned above. In the rightmost plot we see the second surface after it was reparametrized with the homeomorphism on the unit square corresponding to the partial elastic shape registration of the pair of surfaces, a homeomorphism computed based on the optimal diffeomorphism obtained each time (101 times) the Dynamic Programming software was executed for the pair of surfaces, and that because of the simplicity of the surfaces involved and the fact that for the given  $\gamma$  the discretization of the second surface was perturbed only in the  $r$  direction, was always the same diffeomorphism, the diffeomorphism whose graph appears in the rightmost plot in Figure 3.

Finally, we note that with  $\gamma(r,t) = (r^{5/4}, t^{5/4})$ ,  $(r,t) \in [0,1] \times [0,1]$ , the software package was applied on the pair of surfaces in the leftmost plot in Figure 2. The computed elastic shape distance between the two surfaces was 0.0126, the time of execution was 28 seconds, with the **repeat** loop in Procedure DP-surface-min in Section 7 executed 3 times, and the computed optimal rotation matrix for the pair of surfaces was  $\begin{pmatrix} 0 & 1 & 0 \\ 0 & 0 & 1 \\ 1 & 0 & 0 \end{pmatrix}$ . These results were not far from those obtained with the previous  $\gamma$ , however for the current  $\gamma$  the discretization of the second surface was perturbed in both the  $r$  and  $t$  directions. As Procedure

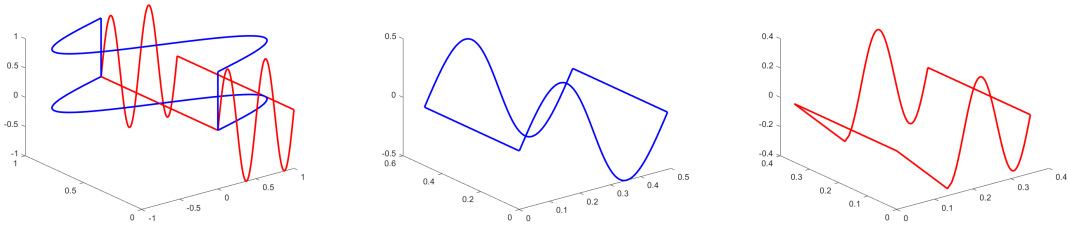


**Fig. 4.** With  $\gamma(r,t) = (r^{5/4}, t)$ ,  $(r,t) \in [0, 1] \times [0, 1]$ , views of boundaries of pair of surfaces in the rightmost plot in Figure 2 before computation of partial elastic shape registration (leftmost plot here), of boundary of optimally rotated first surface (middle plot), and of boundary of optimally reparametrized second surface (rightmost plot) after computations.

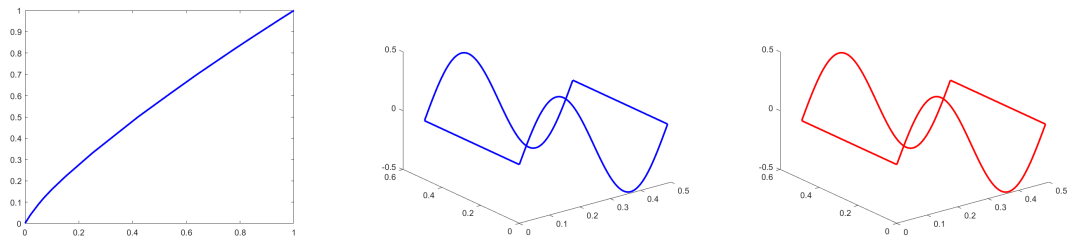


**Fig. 5.** For  $\gamma(r,t) = (r^{5/4}, t^{5/4})$ ,  $(r,t) \in [0, 1] \times [0, 1]$ , views of graph of optimal diffeomorphism computed the 51<sup>st</sup> time the Dynamic Programming software was executed (leftmost plot), of boundary of optimally rotated first surface (middle plot), and of optimally reparametrized second surface (rightmost plot) after computation of partial elastic shape registration.

DP-surface-min is not equipped to handle perturbations in the  $t$  direction, perhaps this was the reason why the computed elastic shape distance between the two surfaces was not exactly zero as in particular the optimal orientation-preserving diffeomorphisms from  $[0, 1]$  onto  $[0, 1]$  computed with the Dynamic Programming software differed slightly from one another, while the computed elastic shape distances between the curves in 3–dimensional space used as input to the software differed from one another as well and were not exactly close to zero. The graph of the optimal diffeomorphism computed the 51<sup>st</sup> time the Dynamic Programming software was executed is shown in Figure 5 together with results of the partial elastic shape registration of the pair of surfaces. It should be noted here that perhaps as long as the second surfaces we have chosen for testing the software are perturbed in the same manner in the  $r$  direction, it is likely the graphs of the optimal diffeomorphisms computed with the Dynamic Programming software will tend to resemble one another regardless of the surfaces involved.

The next results that follow were obtained from applications of our software package on discretizations of surfaces in 3–dimensional space of the helicoid kind. Given  $k$ , a positive integer, one type of surface to which we refer as a surface of the helicoid kind (type 1) is

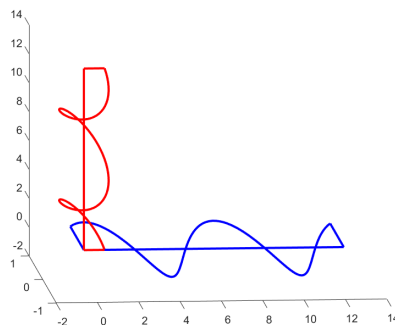


**Fig. 6.** Boundaries of two surfaces of similar shape of the helicoid kind for  $k = 4$ , type 1 in red, type 2 in blue.

defined by

$$x(r,t) = r \cos k\pi t, \quad y(r,t) = r \sin k\pi t, \quad z(r,t) = k\pi t, \quad (r,t) \in [0, 1] \times [0, 1],$$

and another one (type 2) by

$$x(r,t) = k\pi t, \quad y(r,t) = r \cos k\pi t, \quad z(r,t) = r \sin k\pi t, \quad (r,t) \in [0, 1] \times [0, 1],$$

the former a rotation of the latter by applying the rotation matrix  $\begin{pmatrix} 0 & 1 & 0 \\ 0 & 0 & 1 \\ 1 & 0 & 0 \end{pmatrix}$  on the latter, thus of similar shape.

A plot depicting two surfaces (actually their boundaries) of similar shape of the helicoid kind for  $k = 4$  is shown in Figure 6. (Note that in the plot there, the  $x$ -,  $y$ -,  $z$ - axes are not always to scale relative to one another). The two surfaces being of similar shape, clearly the elastic shape distance between them is exactly zero, and the hope was once again that the execution of our software package applied on these two surfaces would produce an elastic shape distance between them equal or close to zero. The type 2 surface of the helicoid kind in the plot (in blue) was considered to be the first surface in the plot. The other surface in the plot (in red) is a type 1 surface of the helicoid kind and was considered to be the second surface in the plot.

With  $\gamma(r,t) = (r^{5/4}, t)$ ,  $(r,t) \in [0, 1] \times [0, 1]$ , the two surfaces in the plot were then discretized as described above and a partial elastic shape registration of the two surfaces and the elastic shape distance between them associated with the partial registration were then computed through the execution of our software package. Again we note that for this particular  $\gamma$ , the discretization of the second surface was perturbed only in the  $r$  direction which as pointed out above made the software package more likely to succeed. The computed distance was 0.0002, which, as hoped for, was close enough to zero. The time of execution was 15 seconds with the **repeat** loop in Procedure DP-surface-min in Section 7 executed 2 times. The computed optimal rotation matrix for the pair of surfaces was  $\begin{pmatrix} 0 & 1 & 0 \\ 0 & 0 & 1 \\ 1 & 0 & 0 \end{pmatrix}$ . As was

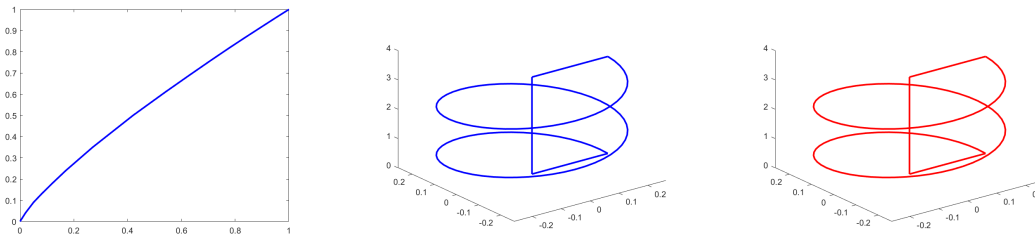


**Fig. 7.** For  $\gamma(r,t) = (r^{5/4}, t)$ ,  $(r,t) \in [0, 1] \times [0, 1]$ , views of graph of optimal diffeomorphism computed each time the Dynamic Programming software was executed on pair of surfaces (leftmost plot), of boundary of optimally rotated first surface (middle plot), and of optimally reparametrized second surface (rightmost plot) after computation of partial elastic shape registration.

the case for surfaces of the sine kind, once again essentially the same solution was obtained each time the Dynamic Programming software was executed as essentially the same two curves in 3–dimensional space contained in the surfaces in the  $r$  direction were used each time as input to the software (the same two curves in the sense that given a pair of curves used as input, the two curves had the same shape and that shape was the same shape of each curve in any other pair used as input to the Dynamic Programming software). In particular, essentially the same optimal orientation-preserving diffeomorphism from  $[0, 1]$  onto  $[0, 1]$  was computed each time together with the same elastic shape distance close to zero between the two curves in 3–dimensional space used as input to the software. The graph of this optimal diffeomorphism is shown in Figure 7 together with results of the partial elastic shape registration of the pair of surfaces.

Finally, we note that with  $\gamma(r,t) = (r^{5/4}, t^{5/4})$ ,  $(r,t) \in [0, 1] \times [0, 1]$ , the software package was applied again on the pair of surfaces. The computed elastic shape distance between the two surfaces was 0.0796, the time of execution was 19 seconds, with the **repeat** loop in Procedure DP-surface-min in Section 7 executed 2 times, and the computed optimal rotation matrix for the pair of surfaces was approximately  $\begin{pmatrix} .028 & .762 & .647 \\ -.029 & -.646 & .763 \\ .999 & -.040 & .004 \end{pmatrix}$ . These results were not as good as those obtained with the previous  $\gamma$  but still acceptable considering that for the current  $\gamma$  the discretization of the second surface was perturbed in both the  $r$  and  $t$  directions. As mentioned above Procedure DP-surface-min is not equipped to handle perturbations in the  $t$  direction, so perhaps this was the reason why the computed elastic shape distance between the two surfaces was not exactly zero as in particular the optimal orientation-preserving diffeomorphisms from  $[0, 1]$  onto  $[0, 1]$  computed with the Dynamic Programming software differed slightly from one another, while the computed elastic shape distances between the curves in 3–dimensional space used as input to the software differed from one another as well and were not exactly close to zero. This inability to handle perturbations in the  $t$  direction may have also affected the computation of the optimal rotation matrix. The graph of the optimal diffeomorphism computed the 51<sup>st</sup> time the Dynamic Pro-

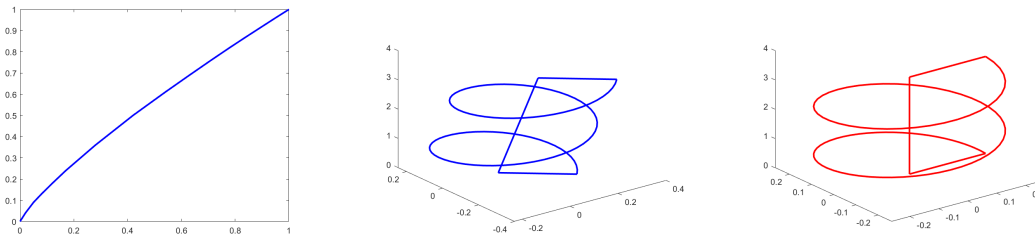


**Fig. 8.** For  $\gamma(r,t) = (r^{5/4}, t^{5/4})$ ,  $(r,t) \in [0,1] \times [0,1]$ , views of graph of optimal diffeomorphism computed the 51<sup>st</sup> time the Dynamic Programming software was executed (leftmost plot), of boundary of optimally rotated first surface (middle plot), and of optimally reparametrized second surface (rightmost plot) after computation of partial elastic shape registration.

gramming software was executed is shown in Figure 8 together with results of the partial elastic shape registration of the pair of surfaces. Once again we note that perhaps as long as the second surfaces we have chosen for testing the software are perturbed in the same manner in the  $r$  direction, it is likely the graphs of the optimal diffeomorphisms computed with the Dynamic Programming software will tend to resemble one another regardless of the surfaces involved.

The final results that follow were obtained from applications of our software package on discretizations of surfaces in 3–dimensional space that are actually graphs of 3–dimensional functions based on the product of the cosine and sine functions. One surface of this kind to which we refer as a surface of the cosine-sine kind (type 1) is defined by

$$x(r,t) = r, \quad y(r,t) = t, \quad z(r,t) = (\cos 0.5\pi r)(\sin 0.5\pi t), \quad (r,t) \in [0,1] \times [0,1],$$

and another one (type 2) by

$$x(r,t) = (\cos 0.5\pi r)(\sin 0.5\pi t), \quad y(r,t) = r, \quad z(r,t) = t, \quad (r,t) \in [0,1] \times [0,1],$$

the former a rotation of the latter by applying the rotation matrix  $\begin{pmatrix} 0 & 1 & 0 \\ 0 & 0 & 1 \\ 1 & 0 & 0 \end{pmatrix}$  on the latter, thus of similar shape.

A plot depicting two surfaces (actually their boundaries) of similar shape of the cosine-sine kind is shown in Figure 9. (Note that in the plot there, the  $x$ –,  $y$ –,  $z$ – axes are not always to scale relative to one another). The two surfaces being of similar shape, clearly the elastic shape distance between them is exactly zero, and the hope was once again that the execution of our software package applied on these two surfaces would produce an elastic shape distance between them equal or close to zero. The type 2 surface of the cosine-sine kind in the plot (in blue) was considered to be the first surface in the plot. The other surface in the plot (in red) is a type 1 surface of the cosine-sine kind and was considered to be the second surface in the plot.



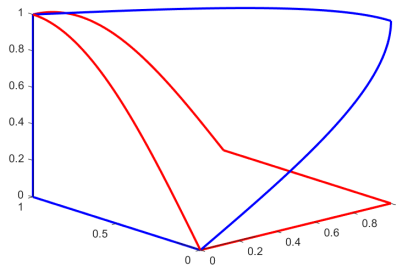


**Fig. 9.** Boundaries of two surfaces of similar shape of the cosine-sine kind, type 1 in red, type 2 in blue.

With  $\gamma(r,t) = (r^{5/4}, t)$ ,  $(r,t) \in [0,1] \times [0,1]$ , the two surfaces in the plot were then discretized as described above and a partial elastic shape registration of the two surfaces and the elastic shape distance between them associated with the partial registration were then computed through the execution of our software package. Again we note that for this particular  $\gamma$ , the discretization of the second surface was perturbed only in the  $r$  direction which as pointed out above made the software package more likely to succeed. The computed distance was 0.0002, which, as hoped for, was close enough to zero. The time of execution was 22 seconds with the **repeat** loop in Procedure DP-surface-min in Section 7 executed 3 times. The computed optimal rotation matrix for the pair of surfaces was essentially  $\begin{pmatrix} 0 & 1 & 0 \\ 0 & 0 & 1 \\ 1 & 0 & 0 \end{pmatrix}$ . It should be noted here that the type 1 surface of the cosine-sine kind satisfies that given  $t_1, t_2, 0 \leq t_1 < t_2 \leq 1$ , then the two 3-dimensional curves in the surface obtained by fixing  $t$  to  $t_1$  and  $t$  to  $t_2$ , have different shapes. In spite of this, the optimal orientation-preserving diffeomorphisms from  $[0,1]$  onto  $[0,1]$  computed with the Dynamic Programming software for the given  $\gamma$ , although differing from one another, differed only very slightly, while the computed elastic shape distances between the curves in 3-dimensional space used as input to the software were all very close to zero. The graph of the optimal diffeomorphism computed the 51<sup>st</sup> time the Dynamic Programming software was executed is shown in Figure 10 together with results of the partial elastic shape registration of the pair of surfaces.

Finally, we note that with  $\gamma(r,t) = (r^{5/4}, t^{5/4})$ ,  $(r,t) \in [0,1] \times [0,1]$ , the software package was applied again on the pair of surfaces. The computed elastic shape distance between the two surfaces was 0.0143, the time of execution was 23 seconds, with the **repeat** loop in Procedure DP-surface-min in Section 7 executed 3 times, and the computed optimal rotation matrix for the pair of surfaces was approximately  $\begin{pmatrix} -.043 & .999 & .026 \\ -.035 & -.028 & .999 \\ .998 & .042 & .036 \end{pmatrix}$ . These results although not as good as those obtained with the previous  $\gamma$  were still acceptable considering once again that for the current  $\gamma$  the discretization of the second surface was perturbed in both the  $r$  and  $t$  directions. Again as mentioned above Procedure DP-surface-min is not

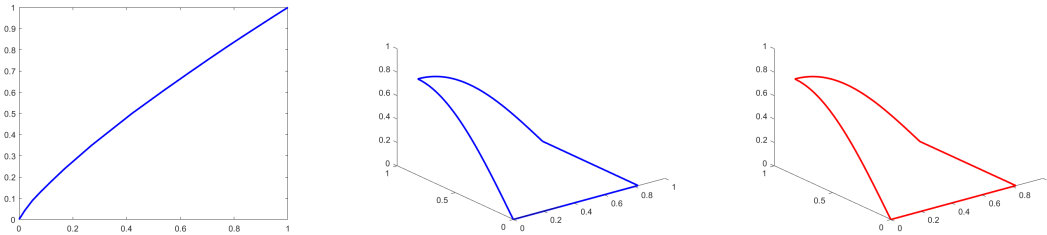


**Fig. 10.** For  $\gamma(r,t) = (r^{5/4}, t)$ ,  $(r,t) \in [0, 1] \times [0, 1]$ , views of graph of optimal diffeomorphism computed the 51<sup>st</sup> time the Dynamic Programming software was executed on pair of surfaces (leftmost plot), of boundary of optimally rotated first surface (middle plot), and of optimally reparametrized second surface (rightmost plot) after computation of partial registration.

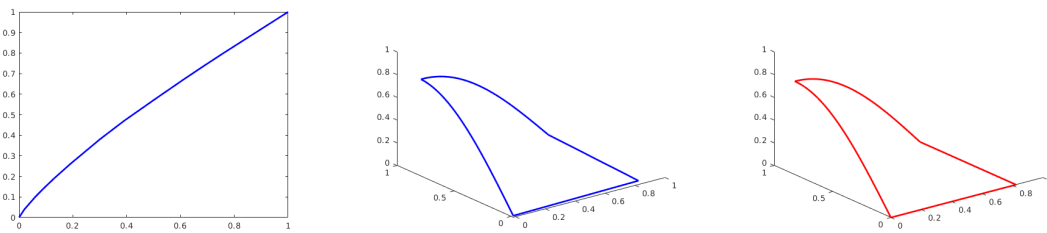


**Fig. 11.** For  $\gamma(r,t) = (r^{5/4}, t^{5/4})$ ,  $(r,t) \in [0, 1] \times [0, 1]$ , views of graph of optimal diffeomorphism computed the 51<sup>st</sup> time the Dynamic Programming software was executed (leftmost plot), of boundary of optimally rotated first surface (middle plot), and of optimally reparametrized second surface (rightmost plot) after computation of partial elastic shape registration.

equipped to handle perturbations in the  $t$  direction, so perhaps this was the reason why the computed elastic shape distance between the two surfaces was not exactly zero as in particular the optimal orientation-preserving diffeomorphisms from  $[0, 1]$  onto  $[0, 1]$  computed with the Dynamic Programming software differed slightly from one another, while the computed elastic shape distances between the curves in 3-dimensional space used as input to the software differed from one another as well and were not exactly close to zero. The graph of the optimal diffeomorphism computed the 51<sup>st</sup> time the Dynamic Programming software was executed is shown in Figure 11 together with results of the partial elastic shape registration of the pair of surfaces. Once again we note that perhaps as long as the second surfaces we have chosen for testing the software are perturbed in the same manner in the  $r$  direction, it is likely the graphs of the optimal diffeomorphisms computed with the Dynamic Programming software will tend to resemble one another regardless of the surfaces involved.

## 9. Summary

In this paper we have presented an algorithm for computing, using Dynamic Programming, a partial elastic shape registration of two simple surfaces in 3–dimensional space together with the elastic shape distance between them associated with the partial registration. The algorithm we have presented minimizes a distance function of the surfaces in terms of rotations of one of the surfaces and a special subset of the set of reparametrizations of the other surface, the optimization over reparametrizations based on the computation, using Dynamic Programming, of the elastic shape registration of pairs of simple curves in 3–dimensional space contained in the surfaces. This algorithm does not necessarily compute an optimal elastic shape registration of the surfaces together with the exact elastic shape distance between them, but perhaps a registration and a distance closer to optimal than those obtained with an algorithm based on a gradient approach over the entire set of reparametrizations of one of the surfaces. In fact we propose that when computing the elastic shape registration of two simple surfaces and the elastic shape distance between them with an algorithm based on a gradient approach for optimizing over the entire set of reparametrizations of one of the surfaces, to use as the input initial solution the rotation and the reparametrization computed with our proposed algorithm. Finally, we note, promising results from computations with the implementation of our methods applied on three simple kinds of 3–dimensional surfaces, have been presented in this paper. A link to the software package, etc., has been given as well.

## References

- [1] Bernal, J., Dogan, G., Hagwood, C. R.: Fast Dynamic Programming for Elastic Registration of Curves. Proceedings of DIFF-CVML workshop, CVPR 2016, Las Vegas, Nevada. (2016)
- [2] Bernal, J.: Shape Analysis, Lebesgue Integration and Absolute Continuity Connections. NISTIR 8217 (2018).
- [3] Bernal, J., Lawrence, J.: Characterization and Computation of Matrices of Maximal Trace Over Rotations. Journal of Geometry and Symmetry in Physics. 53 (2019).
- [4] Bernal, J., Lawrence, J., Dogan, G., Hagwood, C. R.: On Computing Elastic Shape Distances between Curves in d-dimensional Space. NIST Technical Note 2164 (2021)
- [5] Dogan, G., Bernal, J., Hagwood, C. R.: FFT-based alignment of 2d closed curves with application to elastic shape analysis. Proceedings of the 1st DIFF-CV Workshop, British Machine Vision Conference, Swansea, Wales, UK. September 2015.
- [6] Jermyn, I. H., Kurtek, S., Klassen, E., and Srivastava, A.: Elastic shape matching of parameterized surfaces using square root normal fields. Proceedings of the 12th European Conference on Computer Vision (ECCV'12), Volume V, pp. 804–817. Springer, Berlin (2012)
- [7] Joshi, S. H., Klassen, E., Srivastava, A., and Jermyn, I. H.: A novel representation for riemannian analysis of elastic curves in  $R^n$ . Proceedings of the IEEE Conference on Computer Vision and Pattern Recognition (CVPR), Minneapolis, MN. June 2007.
- [8] Kabsch, W.: A solution for the best rotation to relate two sets of vectors. Acta Crystallographica Section A: Crystal Physics. 32(5): 922-923 (1976).
- [9] Kabsch, W.: A discussion of the solution for the best rotation to relate two sets of vectors. Acta Crystallographica Section A: Crystal Physics. 34(5): 827-828 (1978).
- [10] Kurtek, S., Klassen, E., Ding, Z., Srivastava, A.: A novel riemannian framework for shape analysis of 3D objects. Proceedings of the IEEE Conference on Computer Vision and Pattern Recognition (CVPR), San Francisco, CA. June 2010.
- [11] Lawrence, J., Bernal, J., Witzgall, C.: A Purely Algebraic Justification of the Kabsch-Umeyama Algorithm. Journal of Research of the National Institute of Standards and Technology. 124 (2019).
- [12] Lay D., Lay S. and McDonald J.: *Linear Algebra and its Applications*, 5th edition, Pearson Education, Boston 2016.
- [13] Salvador, S., Chan, P.: FastDTW: Toward Accurate Dynamic Time Warping in Linear Time and Space. 3rd Wkshp. on Mining Temporal and Sequential Data, ACM KDD '04. (2004)
- [14] Srivastava, A., Klassen, E. P.: Functional and Shape Data Analysis. New York: Springer. (2016)
- [15] Srivastava, A., Klassen, E. P., Joshi, S. H., Jermyn, I. H.: Shape Analysis of Elastic Curves in Euclidean Spaces. IEEE Trans. Pattern Analysis and Machine Intelligence. 33(7): 1415-1428 (2011).
- [16] Umeyama, S.: Least-Squares Estimation of Transformation Parameters Between Two

Point Patterns. *IEEE Trans. Pattern Analysis and Machine Intelligence*. 13(4): 376-380 (1991).